

Paterno R. Castillo · Philip E. Janney
Renato U. Solidum

Petrology and geochemistry of Camiguin Island, southern Philippines: insights to the source of adakites and other lavas in a complex arc setting

Received: 27 February 1998 / Accepted: 27 August 1998

Abstract Camiguin is a small volcanic island located 12 km north of Mindanao Island in southern Philippines. The island consists of four volcanic centers which have erupted basaltic to rhyolitic calcalkaline lavas during the last ~400 ka. Major element, trace element and Sr, Nd and Pb isotopic data indicate that the volcanic centers have produced a single lava series from a common mantle source. Modeling results indicate that Camiguin lavas were produced by periodic injection of a parental magma into shallow magma chambers allowing assimilation and fractional crystallization (AFC) processes to take place. The chemical and isotopic composition of Camiguin lavas bears strong resemblance to the majority of lavas from the central Mindanao volcanic field confirming that Camiguin is an extension of the tectonically complex Central Mindanao Arc (CMA). The most likely source of Camiguin and most CMA magmas is the mantle wedge metasomatized by fluids dehydrated from a subducted slab. Some Camiguin high-silica lavas are similar to high-silica lavas from Mindanao, which have been identified as “adakites” derived from direct melting of a subducted basaltic crust. More detailed comparison of Camiguin and Mindanao adakites with silicic slab-derived melts and magnesian andesites from the western Aleutians, southernmost Chile and Batan Island in northern Philippines indicates that the Mindanao adakites are not pure slab melts. Rather, the CMA adakites are similar to Camiguin high-silica lavas which are products of an

AFC process and have negligible connection to melting of subducted basaltic crust.

Introduction

The Philippine archipelago (Fig. 1), a complex amalgamation of geologic terranes from various locations along the western Pacific margin, is bordered by several active subduction zones (e.g., Hamilton 1979; Hall 1996). Magmatism in the northern and central Philippines is mainly confined to two parallel zones of arc volcanism running along the length of the archipelago at its eastern and western edges (these zones are henceforth termed the eastern and western arcs, respectively). The eastern arc, which includes the Bicol Arc of southeastern Luzon (e.g., Newhall 1979) and arc volcanoes on Leyte and eastern Mindanao (Sajona et al. 1993, 1997), is associated with the Philippine Trench where the Philippine Sea Plate, with a modest cover of pelagic sediment, is being subducted toward the west. The western arc, which includes the Taiwan-Luzon Arc system (Defant et al. 1989) and arc volcanoes on Mindoro, Panay, Negros (von Biedersee and Pichler 1995), and southwestern Mindanao (Sajona et al. 1996), is associated with the discontinuous Manila, Negros, and Cotabato trenches where South China, Sulu, and Celebes Sea crust, all with a thick cover of terrigenous sediment, are respectively being subducted toward the east. The diverse conditions under which arc volcanism occurs have made the northern Philippines a valuable natural laboratory for studying the impact of different tectonic environments (i.e., arc-continent collision in southwestern Luzon – e.g., Defant et al. 1988; Förster et al. 1990) and varying types and amounts of subducted material (e.g., Mukasa et al. 1987; Knittel and Defant 1988; McDermott et al. 1993; Castillo 1996) on the petrogenesis and geochemistry of arc lavas.

P.R. Castillo (✉) · P.E. Janney
Scripps Institution of Oceanography, University of California,
San Diego, La Jolla, CA 92093-0220, USA;
Tel.: (619) 534-0383; Fax: (619) 534-0784;
E-mail: pcastillo@ucsd.edu

R.U. Solidum
Philippine Institute of Volcanology and Seismology,
Quezon City, Philippines

Editorial responsibility: T. L. Grove

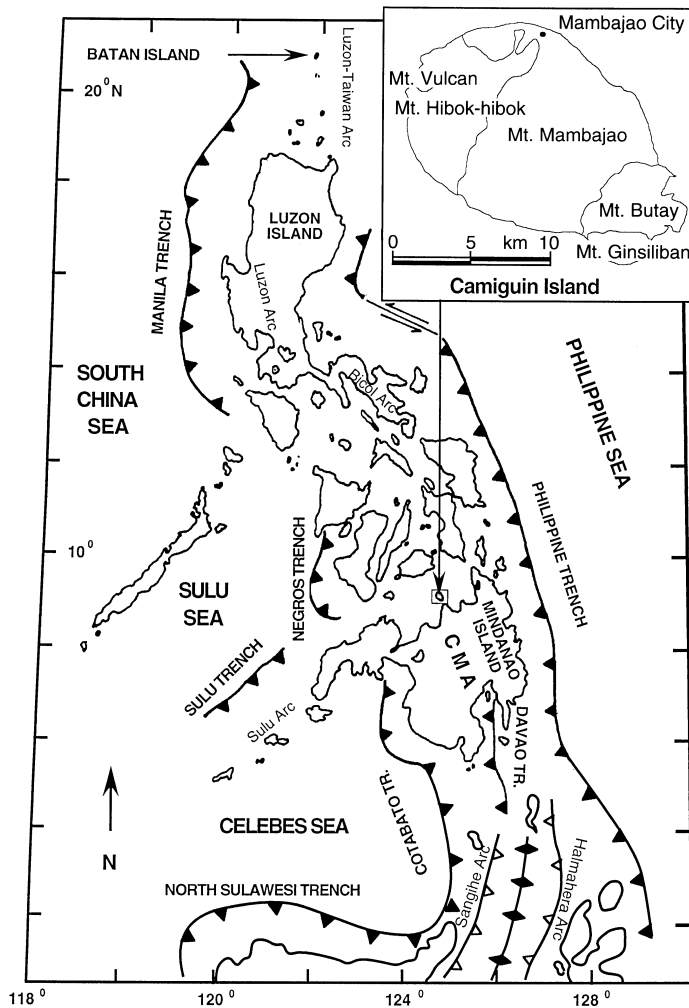


Fig. 1 Map of the Philippines showing major tectonic features (adapted from Hamilton 1979). *Inset* shows simple geologic map of Camiguin Island showing the four major volcanic centers and their geographic coverage (adapted from Punongbayan and Solidum 1985)

The tectonic setting of the southern Philippines is more complex than that of the northern Philippines because of the presence of three and possibly four arc systems in the region (e.g., Moore and Silver 1983; Hawkins et al. 1985; Pubellier et al. 1991). In addition to the eastern and western arcs, Neogene to Quaternary arc volcanoes of the Sulu Arc and Central Mindanao Arc (CMA) exist on Mindanao Island (Fig. 1). The Sulu Arc, on the western peninsular extension of the island, is associated with the subduction of the Sulu Sea crust along the Sulu Trench toward the southeast. On the other hand, the CMA is located roughly halfway between the eastern and western Philippine arcs and is the most areally extensive field of active volcanoes in the Philippines (Sajona et al. 1993). Thus the arc association as well as the cause and source(s) of magmatism in the CMA are uncertain. Several seismic studies, however, have suggested that the CMA is associated with remnants of the subducted Molluca Sea Plate underneath the southern portion of Mindanao Island (Besana et al.

1997; Pubellier et al. 1991; Acharya and Aggarwal 1980). Moreover, reconnaissance petrologic investigations of the CMA reported the presence of lavas derived from melting of the basaltic portion of the subducted Molluca Sea Plate (e.g., Sajona et al. 1993, 1994, 1997; Maury et al. 1996). Although melts of the subducted basaltic crust, collectively termed “adakites” by Drummond and Defant (1990; see also Defant and Drummond 1990), may have been common in the Archean as trondhjemitic-tonalitic granitoids (e.g., Martin 1986; Drummond and Defant 1990), their reported presence in numerous Cenozoic arc settings (e.g., Defant et al. 1992; Drummond et al. 1996) is controversial. Many of the purported Cenozoic adakites may have other origins (e.g., Atherton and Petford 1993; Kay and Kay 1993; Peacock et al. 1994).

In this paper, we present a detailed major element, trace element and Sr-Nd-Pb isotopic investigation of the Pliocene–Quaternary volcanoes of Camiguin Island, the youngest and northernmost volcanic centers in the CMA (Corpuz 1992; Sajona et al. 1993, 1994, 1997). Our primary objectives are to characterize the source composition and fractionation processes that produced Camiguin lavas, and to use these data to constrain the source and melt generation processes that gave rise to adakite lavas here and elsewhere in the CMA. Although the previous CMA petrologic investigations have been valuable for establishing the general geochemical characteristics of the whole arc, their reconnaissance nature cannot provide the kind of in-depth petrogenetic information furnished by an analysis of the entire lava series of one of the volcanic centers in the CMA.

Geologic setting and samples

Camiguin is a small (292 km²) oblate island composed of four exposed stratovolcanoes and a few subsidiary edifices (Fig. 1). The island is situated on a low submarine ridge that extends ~12 km from a peninsula formed by a large volcano of the CMA in north-central Mindanao. The Camiguin volcanoes are aligned northwest-southeast, roughly parallel to the alignment of CMA volcanoes on Mindanao. Field relations (Punongbayan and Solidum 1985) and K-Ar dating (Sajona et al. 1997) reveal that volcanism started with the eruption of Camiguin Tanda volcano (now buried) on the floor of the Mindanao (now Bohol) Sea (Punongbayan and Solidum 1985). Since then, volcanism has progressed toward the northwest by formation of Mts. Butay (0.34 Ma) and Ginsiliban, the oldest and second oldest exposed volcanoes on Camiguin. These relatively small edifices are mainly composed of basaltic to dacitic lavas. Mt. Mambajao, the second youngest (< 100 ka) and largest volcano, is located in the center of the island. Hibok-hibok, located in the northwest, is the youngest and only active volcano. Its last eruptive period started in 1948 and culminated with a Peléan eruption in 1951 that claimed 3,000 lives. Mt. Vulcan is a parasitic dome structure on the northwestern flank of Hibok-hibok volcano. These latter three edifices are mainly andesitic to rhyolitic in composition.

The materials analyzed for this study include 44 lavas sampled from all the volcanic centers and major edifices on the island, and one gabbroic xenolith from Mt. Butay. All of these were analyzed for major oxides and selected trace elements. Rare earth element determinations, mineral analyses and isotopic measurements were conducted on a smaller number of representative samples which were selected based on major element and petrographic data.

Analytical techniques

Major element and Rb, Ba, Sr, Zr, Y, V, Nb and Ni analyses were performed by X-ray fluorescence spectrometry (XRF) on a wavelength-dispersive Phillips instrument at the Scripps Institution of Oceanography (SIO). Determination of major element oxides was conducted on fused disks (0.5 g sample: 2.5 g LiBO₂ flux) following the method of Norrish and Hutton (1969). Trace elements were measured using pressed powder pellets (3 g sample: 1 g methyl cellulose) following the method of Norrish and Chappell (1977).

All mineral analyses were conducted on a Cameca CAMEBAX microprobe equipped with three wavelength-dispersive spectrometers at SIO using parameters described by Janney et al. (1995).

Rare earth element (REE) determinations were performed by inductively coupled plasma mass spectrometry (ICP-MS) on a VG PlasmaQuad 2+ instrument at SIO. Rock powders (0.014 g) were digested using the procedure described in Janney and Castillo (1996), diluted by a factor of 1000 in a 1% HNO₃ solution containing 100 ppb of ¹¹⁵In as an internal standard. The accuracy and precision of the REE measurements were monitored by repeated analysis of the rock standards AGV-1 and BCR-1 and are within 3% relative standard deviation (RSD) for all REE.

The Sr, Nd, and Pb isotope measurements were done at the Department of Terrestrial Magnetism of the Carnegie Institution of Washington using the well-established procedure there (e.g., Walker et al. 1989; Castillo et al. 1991). About 200 mg of rock powders were dissolved in teflon beakers and then passed through small HBr ion exchange columns to collect Pb. The residues from Pb extraction were collected and dried, and less than half (~75 mg) of them were passed through primary cation exchange columns to collect Sr and the REE. Finally, Nd was separated from the rest of the REE by passing the REE cuts through small EDTA ion exchange columns. The Pb and Sr isotope measurement was done using a five-collector VG 354 thermal ionization instrument. The Nd isotope measurement was done in oxide form using a home-built, 15-inch radius thermal ionization instrument.

Results

Petrography and mineral chemistry

Sampled lava types range from basalts (49 wt% SiO₂) to rhyolites (75 wt% SiO₂), although andesites and basaltic andesites dominate (Table 1 and Fig. 2). Almost all lavas are porphyritic, with the volume proportion of phenocrysts generally increasing with differentiation, from 10–15 vol.% in basalts to 30–60 vol.% in the more evolved andesites and dacites. The lavas tend to be sparsely vesicular and most have groundmasses composed primarily of plagioclase laths, oxide minerals (mainly titanomagnetite) and glass. The samples are generally fresh, although olivine has been severely iddingtonized in some basalts, basaltic andesites and the Mt. Butay gabbro xenolith.

Olivine (Fo_{68–85}) dominates the phenocryst assemblages of the most magnesian basalt (sample B016 from Mt. Butay), but it is only a minor phase in the other basalts and basaltic andesites, where it commonly displays resorption rims. In these lavas, plagioclase, clinopyroxene and orthopyroxene (in decreasing order of abundance) are the major phenocryst phases, with the relative plagioclase content generally increasing with the extent of differentiation (see Table 2 for representative

mineral analyses). Hornblende appears as another major mafic phase in the more evolved andesites, as well as in dacites and rhyolite. Pyroxenes are rare in these differentiated lavas and commonly show rounded or resorbed edges when they are present, as do the rare hornblende phenocrysts which appear in the less evolved andesites. The larger plagioclase phenocrysts in Camiguin lavas almost always show pronounced oscillatory zoning and the An contents of zones within single phenocrysts may vary up to 15%, although cores are generally more calcic than rims. Clinopyroxene phenocrysts are also commonly zoned, often displaying classic “hourglass” sector zoning patterns. Most orthopyroxenes are bronzitic and all fall within a narrow compositional range (En_{69–73}). Two-pyroxene thermometry (Lindsley 1983) yields crystallization temperatures of 950–1100 °C (for pressures of 1 atm to 5 kbar) for lavas containing both pyroxenes.

In summary, the textural characteristics and complexly zoned minerals of Camiguin lavas suggest periodic mixing of less and more evolved magmas, perhaps inside long-lived magma chambers. This scenario would result in variably differentiated, highly phyric lavas containing strongly zoned phenocrysts, which may or may not be in equilibrium with their host magmas, similar to those observed.

The Mt. Butay xenolith (sample C011) is a cumulate gabbro comprised of roughly 70 vol.% plagioclase, 25 vol.% clinopyroxene, 5 vol.% olivine and <1 vol.% orthopyroxene. Clinopyroxene grains typically occupy the interstices between large (0.5–3 mm) subhedral plagioclase and small (<0.5 mm) subhedral olivine grains.

Major elements

Camiguin lavas can be characterized as medium-K and calcalkaline (Table 1 and Fig. 2). The ranges of chemical composition and extents of differentiation vary considerably between the four volcanoes. Mt. Butay, from which the most samples were collected, has the most mafic lavas and the greatest compositional range. Mt.

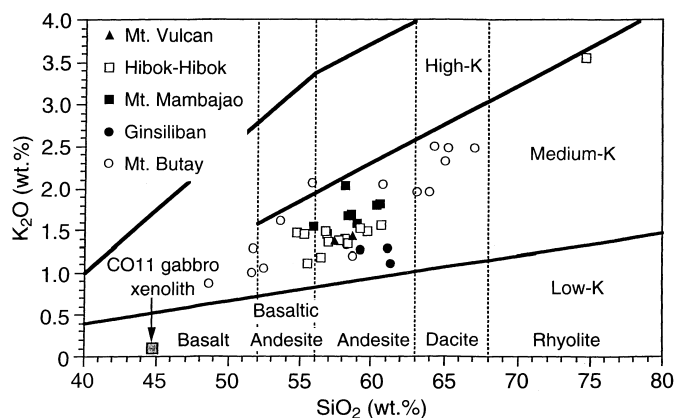


Fig. 2 Plot of K₂O versus SiO₂ for Camiguin lavas. Shaded square symbol represents Mt. Butay gabbroic xenolith

Table 1 Major and trace element compositions of Camiguin Island volcanic rocks

| Sample | Mt. Butay | | | | | | | | | | |
|--------------------------------|-----------|--------|--------|-------|--------|-------|--------|--------|--------|-------|-------|
| | B002 | B003 | B005 | B006 | B007 | B009 | B014 | B015 | B016 | B017 | B018 |
| Major oxides (%) | | | | | | | | | | | |
| SiO ₂ | 58.66 | 63.12 | 60.74 | 52.41 | 58.20 | 51.66 | 51.56 | 63.90 | 48.60 | 65.25 | 53.57 |
| TiO ₂ | 0.61 | 0.52 | 0.52 | 0.78 | 0.65 | 1.28 | 0.80 | 0.42 | 1.04 | 0.37 | 1.13 |
| Al ₂ O ₃ | 18.19 | 17.26 | 18.09 | 18.14 | 18.21 | 16.44 | 18.69 | 18.11 | 16.36 | 17.06 | 18.37 |
| FeO* | 6.57 | 5.38 | 6.04 | 8.62 | 6.60 | 8.78 | 8.92 | 4.86 | 9.99 | 3.93 | 7.71 |
| MnO | 0.14 | 0.14 | 0.14 | 0.16 | 0.13 | 0.17 | 0.17 | 0.11 | 0.18 | 0.13 | 0.14 |
| MgO | 3.66 | 1.85 | 2.70 | 5.07 | 3.88 | 6.86 | 5.37 | 2.34 | 10.03 | 1.75 | 5.63 |
| CaO | 7.27 | 5.93 | 5.97 | 9.78 | 7.62 | 9.35 | 10.72 | 5.13 | 11.48 | 4.75 | 6.58 |
| Na ₂ O | 3.78 | 4.54 | 4.16 | 3.47 | 3.91 | 3.48 | 2.97 | 3.97 | 2.74 | 3.92 | 3.28 |
| K ₂ O | 1.18 | 1.94 | 2.03 | 1.05 | 1.31 | 1.28 | 0.98 | 1.94 | 0.86 | 2.47 | 1.61 |
| P ₂ O ₅ | 0.27 | 0.14 | 0.29 | 0.23 | 0.24 | 0.40 | 0.23 | 0.21 | 0.25 | 0.23 | 0.46 |
| Sum | 100.34 | 100.82 | 100.70 | 99.73 | 100.72 | 99.68 | 100.40 | 100.99 | 101.52 | 99.85 | 98.47 |
| Trace elements (ppm) | | | | | | | | | | | |
| Ni | 19.2 | 7.3 | 3.9 | 24.8 | 23.9 | 106.1 | 24.2 | 10.5 | 125.4 | 1.7 | 101.7 |
| Rb | 27.3 | 19.2 | 43.1 | 14.6 | 44.3 | 14.7 | 50.3 | 21.6 | 43.1 | 50.3 | 21.6 |
| Ba | 255 | 362 | 304 | 171 | 267 | 332 | 162 | 334 | 192 | 401 | 291 |
| Sr | 832 | 850 | 705 | 790 | 704 | 679 | 692 | 769 | 705 | 692 | 769 |
| Zr | 51 | 97 | 71 | 31 | 75 | 52 | 78 | 104 | 71 | 78 | 104 |
| Y | 13.4 | 21.8 | 20.3 | 19.1 | 16.2 | 20.4 | 17.4 | 16.9 | 20.3 | 17.4 | 16.9 |
| V | 151 | 131 | 120 | 249 | 162 | 238 | 276 | 86 | 282 | 60 | 199 |
| Nb | 2 | 5 | 2 | 2 | 4 | 10 | 2 | 2 | 4 | 4 | 7 |
| La | 14.6 | | | | | | | | 9.4 | 17.2 | 20.1 |
| Ce | 18.7 | | | | | | | | 19.5 | 26.3 | 42.5 |
| Pr | 3.7 | | | | | | | | 2.8 | 3.5 | 5.5 |
| Nd | 15.4 | | | | | | | | 13.1 | 14.3 | 24.3 |
| Sm | 3.1 | | | | | | | | 3.1 | 2.7 | 4.6 |
| Eu | 1.2 | | | | | | | | 1.0 | 0.9 | 1.6 |
| Gd | | | | | | | | | 3.4 | 2.8 | 4.4 |
| Tb | 0.45 | | | | | | | | 0.46 | 0.37 | 0.54 |
| Dy | 2.8 | | | | | | | | 2.9 | 2.6 | 3.1 |
| Er | 1.4 | | | | | | | | 1.4 | 1.5 | 1.3 |
| Yb | 1.4 | | | | | | | | 1.3 | 1.6 | 1.1 |
| Lu | 0.21 | | | | | | | | 0.21 | 0.27 | 0.17 |
| Sr/Y | 62 | 39 | 35 | 41 | 44 | 33 | 40 | 45 | 35 | 40 | 45 |
| La/Yb | 11 | | | | | | | | 7 | 11 | 18 |

Hibok-hibok, the youngest volcano, produced the only rhyolite sampled from Camiguin. All Mt. Ginsiliban, Mt. Mambajao, Mt. Vulcan and Mt. Hibok-Hibok lavas, except the rhyolite, fall within a narrow compositional range of 54.5 to 62% SiO₂ (Fig. 2). Because of this narrow interval, there is a significant gap in the Camiguin lava series between the most silicic dacites at 67% SiO₂, and the Hibok-hibok rhyolite, at 75% SiO₂. Camiguin lavas plot on linear or curvilinear trends in most Harker diagrams (Fig. 3) with surprisingly little scatter, suggesting that petrogenetic processes were extremely similar for all volcanoes. This is despite the fact that the lavas are phryic and thus do not represent true liquid compositions. There is also a rough correlation between the relative age of a lava and its composition, in that the oldest lavas at each volcano are generally the most mafic, and younger lavas tend to become increasingly evolved with time.

Trace elements

Trace element abundances are listed in Table 1 together with major element data and are shown graphically in

Figs. 4 to 6. In general, Camiguin lavas are enriched in highly incompatible trace elements such as the light-rare earth elements (REE) and large-ion lithophile elements (LILE) and depleted in high field strength elements (HFSE) relative to other incompatible elements, similar to most calcalkaline arc lavas. In detail, compatible elements Ni and V have strong negative correlations with silica content (Fig. 4). Among the incompatible elements, Rb and Ba display the strongest positive correlations with silica. The behavior of other incompatible trace elements with increasing silica is more complex. Strontium also correlates positively with silica but only up to about 58% SiO₂; it decreases with increasing silica content thereafter, indicating increased plagioclase fractionation in the more evolved lavas. On average, Zr rises with increasing SiO₂, but intersample variation is large particularly among the basaltic andesites and andesites. The large intersample variation of Zr coincides with the preponderance of hornblende as a phenocryst and/or groundmass phase in the more evolved lavas. Since Zr is compatible in hornblende in silicic magmas (e.g., Pearce and Norry 1979; Gill 1981), an argument could be made that the large variation was caused by shifting from a clinopyroxene-dominated to a hornblende-dominated

| Mt. Butay | | | | | Mt. Ginsiliban | | | Mt. Mambajao | | | |
|-----------|-------|-------|--------|------------|----------------|--------|--------|--------------|-------|--------|-------|
| C001 | C002 | C006 | C008 | C011 | G001 | G004 | G006 | M011 | M021 | M022 | M029 |
| | | | | (Xenolith) | | | | | | | |
| 65.04 | 55.76 | 64.21 | 66.96 | 44.77 | 61.31 | 59.18 | 61.05 | 58.51 | 58.98 | 60.53 | 58.30 |
| 0.39 | 0.95 | 0.34 | 0.36 | 0.14 | 0.51 | 0.59 | 0.49 | 0.73 | 0.61 | 0.73 | 0.67 |
| 16.08 | 16.78 | 16.92 | 16.24 | 21.93 | 18.38 | 18.38 | 17.99 | 17.65 | 18.04 | 17.37 | 17.42 |
| 4.33 | 6.23 | 3.75 | 3.70 | 7.23 | 5.52 | 6.53 | 5.54 | 6.19 | 5.99 | 5.88 | 5.86 |
| 0.13 | 0.12 | 0.15 | 0.11 | 0.13 | 0.13 | 0.14 | 0.11 | 0.12 | 0.13 | 0.12 | 0.13 |
| 2.29 | 5.16 | 1.57 | 1.99 | 9.22 | 3.12 | 3.73 | 2.88 | 3.64 | 3.17 | 3.35 | 3.23 |
| 4.99 | 8.10 | 4.66 | 4.36 | 14.98 | 6.83 | 7.56 | 6.13 | 7.18 | 7.04 | 6.31 | 7.03 |
| 3.78 | 3.70 | 4.82 | 4.18 | 1.32 | 3.64 | 3.44 | 4.68 | 5.07 | 4.16 | 4.37 | 4.26 |
| 2.30 | 2.06 | 2.48 | 2.47 | 0.09 | 1.09 | 1.25 | 1.28 | 1.68 | 1.57 | 1.81 | 1.65 |
| 0.09 | 0.50 | 0.23 | 0.06 | 0.02 | 0.22 | 0.27 | 0.23 | 0.26 | 0.26 | 0.31 | 0.28 |
| 99.42 | 99.37 | 99.12 | 100.43 | 99.84 | 100.75 | 101.07 | 100.37 | 101.05 | 99.94 | 100.77 | 98.84 |
| 7.6 | 59.1 | 0.4 | 7.0 | 56.7 | 17.7 | 22.1 | 28.1 | 17.0 | 12.0 | 21.8 | 17.1 |
| 49.9 | 30.9 | 50.3 | 54.1 | 1.5 | 23.4 | 42.2 | 17.9 | 36.6 | 37.4 | 42.3 | 36.3 |
| 350 | 366 | 372 | 362 | 51 | 295 | 249 | 290 | 347 | 305 | | 358 |
| 523 | 1148 | 680 | 506 | 555 | 810 | 653 | 760 | 815 | 895 | 885 | 945 |
| 73 | 99 | 77 | 78 | 3 | 59 | 76 | 39 | 105 | 84 | 91 | 100 |
| 15.4 | 13.6 | 16.9 | 12.8 | 10.8 | 22.3 | 24.5 | 25.3 | 14.3 | 11.8 | 10.1 | 13.2 |
| 110 | 193 | 61 | 83 | 86 | 116 | 151 | 121 | 153 | 135 | 133 | 152 |
| 4 | 11 | 3 | 3 | 1 | 3 | 3 | 2 | 8 | 5 | 8 | 6 |
| | | | | 1.7 | 11.3 | 10.5 | 13.1 | 19.1 | | 21.2 | 22.6 |
| | | | | 1.2 | 21.1 | 20.5 | 22.2 | 36.1 | | 39.3 | 40.0 |
| | | | | 0.4 | 2.8 | 2.8 | 3.3 | 4.4 | | 4.7 | 5.0 |
| | | | | 2.2 | 11.6 | 11.6 | 14.5 | 18.6 | | 18.7 | 19.6 |
| | | | | 0.6 | 2.4 | 2.6 | 2.9 | 3.6 | | 3.5 | 3.8 |
| | | | | 0.4 | 0.9 | 1.0 | 1.1 | 1.2 | | 1.2 | 1.2 |
| | | | | 0.9 | 2.5 | 2.8 | 3.0 | 3.5 | | 3.1 | 3.3 |
| | | | | 0.20 | 0.36 | 0.38 | 0.42 | 0.43 | | 0.35 | 0.44 |
| | | | | 0.8 | 2.3 | 2.5 | 2.7 | 2.7 | | 2.2 | 2.5 |
| | | | | 0.5 | 1.2 | 1.4 | 1.4 | 1.3 | | 0.9 | 1.1 |
| | | | | 0.5 | 1.4 | 1.1 | 1.5 | 1.1 | | 0.9 | 1.1 |
| | | | | 0.15 | 0.21 | 0.22 | 0.24 | 0.17 | | 0.14 | 0.19 |
| 34 | 84 | 40 | 39 | 52 | 36 | 27 | 30 | 57 | 76 | 88 | 71 |
| | | | | 4 | 8 | 9 | 9 | 17 | | 23 | 21 |

fractionating assemblage. The scatter may also be due to the variable presence of trace amounts of zircon, as this mineral is present in other CMA lavas (Sajona et al. 1993, 1994). Yttrium shows a general decrease with increasing silica but with much scatter, again possibly due to variable hornblende fractionation. The C011 cumulate gabbro has extremely low trace element concentrations and because of this, its trace element signature may have been affected by weathering and low-temperature surface alteration, resulting in a very irregular normalized pattern (Figs. 4 and 5).

In the extended trace element diagrams (Fig. 5), Camiguin lavas in general have high concentrations (20–80X primitive mantle) of highly incompatible LILE (Rb, Ba and K) but have lower contents (5–20X primitive mantle) of moderately incompatible trace elements (e.g., middle REE). In detail, the concentrations of highly incompatible LILE increase with increasing fractionation. Among the HFSE, Zr generally increases with increasing fractionation, as mentioned above, but Nb and Ti only initially increase and then decrease above ~63% SiO₂. The complex behavior of the trace element contents of Camiguin lavas is demonstrated by their REE concentration patterns (Fig. 6). The basaltic lavas show light-REE enriched patterns (La/Sm_{ch} > 1.9) similar to

other Philippine mafic arc lavas (e.g., Defant et al. 1988, 1989; Miklius et al. 1991). However, the degree of light-REE enrichment initially increases and then decreases with increasing silica relative to sample BO16. A similar behavior is shown by the middle REE. On the other hand, the heavy REE initially decrease and then continuously increase with increasing silica. The differential behavior of the different REE with increasing silica content causes some of the andesites and dacites to develop U-shaped REE patterns and higher La/Yb ratios than the rest of Camiguin lavas. These geochemical characteristics are similar, although not identical, to the overall decrease of REE with increasing SiO₂ content of some Andean and Mexican arc-related lavas, and which have been attributed to fractionation of amphibole and accessory phases such as titanite and apatite (e.g., Luhr and Carmichael 1980; Kay and Gordillo 1994). Trace amounts of apatite are also present in other CMA lavas (Sajona et al. 1993, 1994).

Sr, Nd and Pb isotopes

The Sr, Nd, and Pb isotopic determinations were made on four, stratigraphically older Camiguin mafic lavas

Table 1 (Continued)

| Sample | Mt. Mambajao | | | Mt. Hibok-Hibok | | | | | | | | |
|--------------------------------|--------------|--------|-------|-----------------|-------|--------|--------|-------|--------|--------|--------|-------|
| | M041 | M043 | M054 | 2H002 | 2H007 | H002 | H003 | H004 | H005 | H008 | H010 | H011 |
| SiO ₂ | 55.86 | 60.38 | 58.15 | 55.29 | 55.45 | 59.70 | 56.38 | 56.85 | 74.59 | 57.73 | 60.63 | 59.13 |
| TiO ₂ | 0.85 | 0.63 | 0.73 | 0.89 | 0.69 | 0.59 | 0.68 | 0.71 | 0.16 | 0.67 | 0.52 | 0.62 |
| Al ₂ O ₃ | 17.51 | 17.94 | 17.95 | 18.17 | 18.64 | 18.08 | 17.87 | 17.71 | 14.97 | 17.68 | 17.87 | 17.87 |
| FeO* | 7.45 | 5.83 | 6.14 | 7.08 | 7.07 | 6.07 | 6.92 | 6.29 | 1.15 | 6.58 | 5.35 | 6.04 |
| MnO | 0.15 | 0.14 | 0.14 | 0.15 | 0.14 | 0.16 | 0.15 | 0.13 | 0.10 | 0.16 | 0.16 | 0.14 |
| MgO | 5.18 | 3.09 | 3.58 | 4.57 | 3.91 | 3.33 | 4.52 | 4.56 | 0.53 | 4.54 | 2.49 | 3.34 |
| CaO | 8.06 | 6.01 | 6.98 | 8.35 | 7.95 | 7.60 | 8.26 | 7.92 | 1.97 | 8.15 | 6.64 | 7.25 |
| Na ₂ O | 3.73 | 4.17 | 3.88 | 4.05 | 3.68 | 4.25 | 3.78 | 3.84 | 4.30 | 3.60 | 4.57 | 3.79 |
| K ₂ O | 1.53 | 1.79 | 2.02 | 1.44 | 1.09 | 1.48 | 1.17 | 1.44 | 3.53 | 1.37 | 1.54 | 1.52 |
| P ₂ O ₅ | 0.31 | 0.22 | 0.36 | 0.52 | 0.35 | 0.28 | 0.27 | 0.30 | 0.03 | 0.29 | 0.29 | 0.27 |
| | 100.64 | 100.19 | 99.94 | 100.50 | 98.96 | 101.54 | 100.01 | 99.76 | 101.33 | 100.76 | 100.06 | 99.96 |
| Ni | 57.7 | 13.1 | 28.5 | 35.8 | 16.3 | 12.6 | 29.6 | 56.7 | n.d. | 29.9 | 6.4 | 14.9 |
| Rb | 33.1 | 42.7 | 45.4 | 31.6 | 21.6 | 35.8 | 25.5 | 29.0 | 79.6 | 31.6 | 36.2 | 32.6 |
| Ba | 336 | 355 | 330 | 356 | 254 | 332 | 267 | 282 | 487 | 301 | 366 | 325 |
| Sr | 840 | 795 | 949 | 1149 | 910 | 912 | 912 | 899 | 397 | 889 | 959 | 884 |
| Zr | 89 | 100 | 124 | 119 | 70 | 98 | 77 | 75 | 95 | 89 | 106 | 77 |
| Y | 16.4 | 16.5 | 14.0 | 14.9 | 14.2 | 15.9 | 15.9 | 14.5 | 10.9 | 16.2 | 16.6 | 14.2 |
| V | 199 | 120 | 172 | 189 | 167 | 138 | 165 | 168 | 155 | 97 | 138 | 138 |
| Nb | 6 | 5 | 8 | 10 | 4 | 8 | 5 | 5 | 3 | 7 | 7 | 6 |
| La | 21.0 | | | 28.3 | | | | 16.4 | 13.9 | 19.3 | 20.5 | |
| Ce | 39.0 | | | 54.6 | | | | 31.9 | 23.3 | 36.9 | 38.9 | |
| Pr | 5.0 | | | 7.1 | | | | 4.0 | 2.6 | 4.6 | 4.6 | |
| Nd | 20.6 | | | 28.8 | | | | 16.6 | 9.1 | 18.6 | 18.2 | |
| Sm | 3.8 | | | 5.0 | | | | 3.2 | 1.5 | 3.6 | 3.3 | |
| Eu | 1.3 | | | 1.6 | | | | 1.1 | 0.5 | 1.2 | 1.1 | |
| Gd | 3.9 | | | 4.4 | | | | 3.2 | 1.5 | 3.5 | | |
| Tb | 0.47 | | | 0.53 | | | | 0.39 | 0.21 | 0.42 | 0.39 | |
| Dy | 2.9 | | | 3.0 | | | | 2.3 | 1.4 | 2.6 | 2.3 | |
| Er | 1.3 | | | 1.3 | | | | 1.1 | 0.9 | 1.3 | 1.1 | |
| Yb | 1.2 | | | 1.2 | | | | 1.1 | 1.2 | 1.3 | 1.2 | |
| Lu | 0.20 | | | 0.19 | | | | 0.16 | 0.21 | 0.19 | 0.20 | |
| Sr/Y | 51 | 48 | 68 | 77 | 64 | 57 | 57 | 62 | 36 | 55 | 58 | 62 |
| La/Yb | 17 | | | 25 | | | | 15 | 12 | 15 | 17 | |

(one from each volcano) and on the gabbro xenolith. The Sr and Nd isotopic determinations were also done on the rhyolite sample (sample H005), the most differentiated and youngest sample from Camiguin. The isotopic ratios are presented in Table 3 and plotted on Fig. 7A to C. For all isotopic systems, the interval volcano variation is small particularly in the Nd system. The rhyolite has slightly higher $^{87}\text{Sr}/^{86}\text{Sr}$ than the other samples but this is most probably due to the longer residence time of the rhyolite lava in the crustal magma chamber than the other more mafic lavas. The gabbro has a somewhat different isotopic composition; it has slightly higher Nd and Pb and lower Sr isotopic ratios than the volcanic rocks.

Also shown on Fig. 7 are fields of data for several arc volcanic localities along the eastern and western Philippines. Compared to other Philippine arc lavas, Camiguin lavas belong to the low $^{87}\text{Sr}/^{86}\text{Sr}$, $^{206}\text{Pb}/^{204}\text{Pb}$, $^{207}\text{Pb}/^{204}\text{Pb}$, $^{208}\text{Pb}/^{204}\text{Pb}$, and high $^{143}\text{Nd}/^{144}\text{Nd}$ group, but do not extend to the extreme composition. In all isotope systems, Camiguin lavas plot near or inside the fields for Leyte Island and eastern Mindanao, which belong to the eastern arc, and Taiwan–Luzon Arc and

Negros Arc, which belong to the western arc. There are only a few isotopic data for the CMA volcanoes (Castillo 1996 and unpublished data; F. Sajona unpublished data). Camiguin lavas completely overlap with the CMA lavas in terms of Sr and Nd isotope ratios, but have slightly higher $^{206}\text{Pb}/^{204}\text{Pb}$ than the CMA lavas.

Discussion

Camiguin Island has been volcanically active since the late Pliocene or early Pleistocene (Punongbayan and Solidum 1985; Sajona et al. 1997) and it is possible that several different melt sources have been involved in producing Camiguin volcanoes over their lifetimes. However, the small interval volcano variations in major and trace element chemistry of Camiguin lavas suggest that they most likely come from a source or sources with a fairly homogeneous composition (e.g., Gill 1981). Moreover, although Camiguin lavas do not represent true liquid compositions, the geochemical coherency shown by these lavas simply suggests that they are produced by a common differentiation process acting

| Mt. Hibok-Hibok | | | | | Mt. Vulcan | | |
|-----------------|-------|--------|--------|---------|------------|--------|--------|
| H012 | H014 | H016 | Hd001 | C03-001 | V005 | V006 | V008 |
| 54.72 | 56.74 | 58.30 | 58.09 | 56.02 | 57.94 | 58.61 | 57.37 |
| 0.82 | 0.67 | 0.67 | 0.61 | 0.69 | 0.64 | 0.64 | 0.62 |
| 17.90 | 18.22 | 18.17 | 18.13 | 18.32 | 17.56 | 17.81 | 17.68 |
| 7.34 | 6.43 | 6.35 | 6.46 | 6.78 | 6.23 | 6.32 | 6.47 |
| 0.16 | 0.16 | 0.15 | 0.16 | 0.14 | 0.16 | 0.15 | 0.16 |
| 4.89 | 3.79 | 3.50 | 3.57 | 4.04 | 3.81 | 3.90 | 4.36 |
| 8.60 | 7.73 | 7.63 | 7.81 | 8.12 | 7.92 | 7.76 | 8.14 |
| 3.84 | 4.29 | 4.37 | 3.83 | 3.83 | 4.07 | 3.91 | 3.86 |
| 1.46 | 1.48 | 1.33 | 1.39 | 1.34 | 1.41 | 1.43 | 1.37 |
| 0.38 | 0.30 | 0.31 | 0.29 | 0.30 | 0.29 | 0.29 | 0.28 |
| 100.11 | 99.82 | 100.79 | 100.33 | 99.58 | 100.02 | 100.84 | 100.29 |
| 29.5 | 16.5 | 16.4 | 12.3 | 23.2 | 19.5 | 21.2 | 30.6 |
| 29.1 | 31.0 | 31.2 | 32.8 | 32.8 | 35.1 | 33.0 | 33.0 |
| 310 | 309 | 308 | 316 | | 316 | 334 | 302 |
| 946 | 916 | 1000 | 907 | 874 | 941 | 898 | 898 |
| 89 | 91 | 90 | 95 | 94 | 91 | 97 | 97 |
| 14.9 | 14.8 | 12.5 | 16.5 | 15.2 | 14.2 | 17.4 | 17.4 |
| 188 | 150 | 137 | 145 | | 159 | 142 | 154 |
| 8 | 6 | 7 | 7 | 6 | 6 | 3 | 5 |
| | | | 19.0 | 15.5 | | 20.8 | 27.1 |
| | | | 35.5 | 30.1 | | 39.2 | 52.9 |
| | | | 4.1 | 3.8 | | 4.8 | 6.9 |
| | | | 16.9 | 16.1 | | 19.0 | 28.0 |
| | | | 3.2 | 3.3 | | 3.6 | 5.0 |
| | | | 1.1 | 1.1 | | 1.2 | 1.6 |
| | | | 3.2 | 2.8 | | 3.4 | 4.6 |
| | | | 0.41 | 0.38 | | 0.42 | 0.54 |
| | | | 2.6 | 2.3 | | 2.6 | 3.0 |
| | | | 1.3 | 1.0 | | 1.3 | 1.3 |
| | | | 1.3 | 1.0 | | 1.2 | 1.2 |
| | | | 0.19 | 0.16 | | 0.20 | 0.20 |
| 64 | 62 | 80 | 55 | 57 | 66 | 52 | 52 |
| | | | 15 | 16 | | 17 | 23 |

upon melts from a fairly homogeneous source. The fact that Camiguin is a fairly young island also helps us to rule out substantial upper crustal contamination that may have affected our petrologic interpretation. Finally, the fairly uniform Sr, Nd and Pb isotopic compositions of Camiguin lavas strongly indicate that Camiguin volcanic centers indeed share a common melt source. Because the range of isotopic values of Philippine arc lavas is quite large (e.g., Mukasa et al. 1994; Castillo 1996), any significant changes in melt source composition would likely have resulted in a much larger intervolcano isotopic variation than is observed.

Interestingly, the gabbro xenolith (sample C011) has an isotopic composition somewhat different from the lava samples (Table 3 and Fig. 7A–C). It has significantly lower Sr and slightly higher Pb isotopic ratios than the lavas. The gabbro also shows chemical attributes that distinguish it from the lavas: its TiO₂, Al₂O₃, FeO*, Na₂O, V and Y values plot well away from the main trend and it has low and irregular trace element concentration pattern (e.g., Figs. 4 and 5). It has a distinctly cumulate texture, but least-squares fractional crystallization models do not support the hypothesis that C011 is an accumulation of minerals fractionated from Camiguin melts because the residual errors are

quite large ($\Sigma r^2 \approx 14$). Based on all these information, sample C011 cannot be a direct product of Camiguin volcanism but most probably is from a cumulate section of the oceanic igneous basement that was stopped by Camiguin lavas on their way to the surface. The similarity of the gabbro's Sr and Nd isotopic ratios with those of the Sulu Sea igneous basement rocks (Fig. 7A) supports this conclusion. However, Sulu Sea basement samples have lower Pb isotopic ratios than C011 (Figs. 7B and C – Spadea et al. 1996; Smith et al. 1991). This appears to complicate the picture, but it is quite possible that the slightly higher Pb isotopic composition of C011 is also an artifact of weathering and surface alteration. Compared to Sr and Nd concentrations (Table 1), the original Pb content of the gabbro cumulate was very low ($\ll 1$ ppm – not shown), and hence, its Pb isotopic composition was highly susceptible to even the slightest alteration and/or metasomatism.

Petrogenesis and volcanic evolution

The wide range of lava types, abundance of phenocrysts in most samples and particularly the coherent geochemical trends of the lavas suggest that fractional

Table 2 Representative microprobe analyses of minerals (*pheno* phenocryst, *cpx* clinopyroxene, *opx* orthopyroxene)

| Mineral | Pyroxene | | | | Plagioclase | | | | |
|--------------------------------|-------------------|----------------------|-------------------|-------------------|----------------|------------------|---------------|---------------|----------------|
| | B016 Cpx pheno | C03-001 Opx pheno | G006 Cpx pheno | G001 Opx pheno | B016 Matrix | C03-001 Pheno | G006 Pheno | B017 Pheno | M022 Matrix |
| SiO ₂ | 48.20 | 54.41 | 51.86 | 52.61 | 48.11 | 51.44 | 51.25 | 49.43 | 56.61 |
| TiO ₂ | 0.86 | 0.21 | 0.00 | 0.16 | 0.08 | 0.04 | 0.06 | 0.02 | 0.02 |
| Al ₂ O ₃ | 6.17 | 0.76 | 1.63 | 2.32 | 32.12 | 30.22 | 29.37 | 31.01 | 27.07 |
| FeO* | 6.89 | 15.62 | 10.66 | 16.17 | 1.17 | 0.77 | 0.76 | 0.46 | 0.22 |
| MnO | 0.14 | 0.55 | 0.44 | 0.75 | 0.03 | 0.01 | 0.02 | 0.01 | 0.03 |
| MgO | 13.88 | 26.79 | 17.05 | 25.24 | 0.01 | 0.07 | 0.08 | 0.03 | 0.00 |
| CaO | 22.82 | 1.51 | 15.64 | 1.16 | 15.08 | 12.96 | 12.42 | 13.79 | 8.89 |
| Na ₂ O | 0.29 | 0.02 | 0.14 | 0.02 | 2.90 | 3.26 | 3.29 | 3.36 | 6.25 |
| K ₂ O | | | | | 0.16 | 0.10 | 0.12 | 0.08 | 0.28 |
| Cr ₂ O ₃ | 0.11 | 0.03 | 0.07 | 0.04 | | | | | |
| sum | 99.36 | 99.90 | 97.49 | 98.47 | 99.66 | 98.87 | 97.37 | 98.19 | 99.37 |

| Mineral | Olivine | | | Hornblende | | | | Oxides | |
|--------------------------------|-----------------|--------------------|---------------------|---------------|---------------|---------------|----------------|----------------|----------------|
| | B-016 Matrix | B-016 Pheno rim | B-016 Pheno core | B017 Pheno | B017 Pheno | M022 Pheno | M022 Matrix | B017 Matrix | B-016 Pheno |
| SiO ₂ | 37.14 | 38.81 | 38.23 | 42.37 | 43.04 | 46.21 | 0.03 | 0.05 | 39.63 |
| TiO ₂ | 0.01 | 0.04 | 0.01 | 1.65 | 1.46 | 1.04 | 6.49 | 4.31 | 0.03 |
| Al ₂ O ₃ | 0.01 | 0.00 | 0.39 | 12.24 | 11.31 | 8.44 | 1.68 | 3.85 | 0.01 |
| FeO* | 23.37 | 18.02 | 13.50 | 12.05 | 13.87 | 12.92 | 88.06 | 89.05 | 13.99 |
| MnO | 0.54 | 0.37 | 0.34 | 0.22 | 0.43 | 0.58 | 0.57 | 0.61 | 0.24 |
| MgO | 37.54 | 41.21 | 42.57 | 13.98 | 12.91 | 14.34 | 1.31 | 1.53 | 45.68 |
| CaO | 0.32 | 0.23 | 0.66 | 11.11 | 11.12 | 10.85 | 0.50 | 0.04 | 0.20 |
| Na ₂ O | 0.00 | 0.00 | 0.01 | 2.19 | 2.06 | 1.24 | 0.01 | 0.00 | 0.00 |
| K ₂ O | 0.01 | 0.00 | 0.00 | 0.46 | 0.49 | 0.44 | 0.01 | 0.00 | 0.03 |
| P ₂ O ₅ | | | | 0.02 | 0.05 | 0.01 | 0.00 | 0.00 | |
| Cr ₂ O ₃ | 0.04 | 0.12 | 0.21 | 0.05 | 0.02 | 0.00 | 0.09 | 0.01 | 0.18 |
| NiO | 0.00 | 0.00 | 0.04 | 0.00 | 0.03 | 0.00 | 0.01 | 0.06 | 0.02 |
| H ₂ O | | | | 2.01 | 2.00 | 2.02 | | | |
| sum | 98.98 | 98.80 | 95.96 | 98.35 | 98.79 | 98.09 | 98.76 | 99.51 | 100.01 |

crystallization was the dominant process controlling the evolution of Camiguin lavas from primary magmas originating from a common source. However, periodic reinjection and autoassimilation of new melt may also have been an important influence and might account for the large proportion of andesites relative to basalts, dacites and rhyolites. In order to illustrate these fractionation processes inferred from the data, we present models for both pure crystal fractionation and melt mixing plus crystal fractionation on representative Camiguin lavas (Table 4). The fractionation calculations were performed using the “GENMIX” least-squares computer program of Le Maitre (1981). For the pure fractionation model, we used sample B016 as the parental liquid composition. Sample B016 is fairly primitive [$\text{MgO} = 10\%$; $\text{Mg}^{2+}/(\text{Mg}^{2+} + \text{Fe}^{2+}) = 0.68$] and has the highest concentration of compatible trace elements ($\text{Ni} = 125$ ppm; $\text{V} = 282$ ppm). Although this sample does not represent a true primary magma, it appears to be a close derivative from one. In the mixing + fractional crystallization model, we used a mix of the primitive basalt B016 and a more silicic lava (e.g., a dacite for model #1, a rhyolite for model #2) as the parent in order to simulate the injection of a mafic parental melt into a chamber containing differentiated

magma. Averaged mineral analyses (Table 2) were used for the compositions of crystallizing phases.

The fractionating mineral assemblages were selected by choosing those phases that produced the smallest residual errors (Σr^2 ; squared oxide weight percent). The residual errors for the pure crystal fractionation models (0.33–0.78) are larger than those for the mixing plus crystallization models (0.071–0.080). In all models the fractionating mineral assemblages agree with the major phenocryst phases observed in thin section. All models required clinopyroxene, plagioclase and olivine fractionation, and hornblende and titanomagnetite were often required as well (see Table 4).

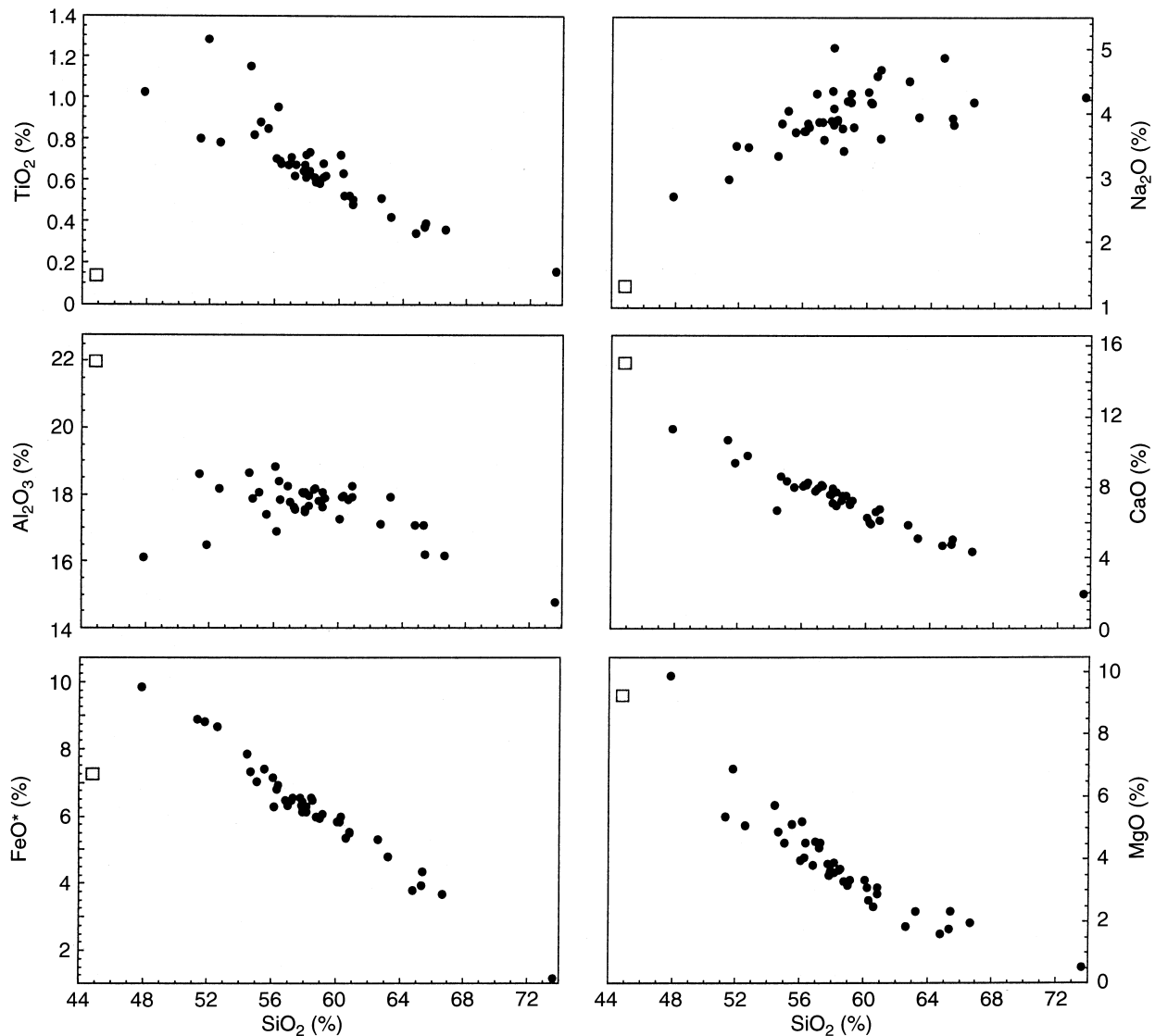
Trace element modeling for selected incompatible trace elements (La, Ce, Nd, Zr, Y, Sr and Rb) was based on the least-squares models discussed above and was conducted using the open system assimilation-fractional crystallization (AFC) technique (Reagan et al. 1987; DePaolo 1981). The pure crystal fractionation models use the basalt B016 as the parent and do not use assimilated or intrusive components in the calculations. The mixing + crystallization models use the “evolved daughter” of the least-squares mixing-crystallization models as the true parent and the B016 basalt as the composition of an intruding magma. The results of the

trace element modeling agree with the least-squares modeling results: models involving mixing plus crystal fractionation produce values that are significantly closer to the actual “daughter” trace element concentrations than those predicted by the pure fractional crystallization models (Table 4). Most errors for the mixing-crystallization models are less than 20% while those for the fractionation models are most often in excess of 50%. Note, however, that the modeled Rb values are high, but these are most probably due to using partition coefficients that are too low for the particular pressure, temperature and P_{H_2O} conditions under which the differentiated magmas crystallized (e.g., Green and Pearson 1985).

In summary, the petrography and chemistry of Camiguin lavas are consistent with an evolution dominantly influenced by fractional crystallization and mixing of magmas that were generated from a common mantle source. Least-squares and AFC models also indicate that mixing of primitive and evolved melts cou-

pled with moderate crystal fractionation produce realistic major and trace element concentrations in the differentiated lavas. Based on these results, we propose that the magmatic evolution of Camiguin lavas involves the initial emplacement of a mafic parental melt into a shallow magma chamber (most Camiguin lavas plot on the 2 kbar fractionation trend of Baker (1987) using the calculation procedure of Baker and Eggler (1983)). The melt begins crystallizing soon after emplacement, but a small portion of it erupts at the surface to form the oldest, most mafic lavas. The crystallization of the melt inside the chamber is punctuated by a series of injection of new batches of parental melt which mixes with the fractionating magma. The arrival of new parental melt in the magma chamber probably triggers volcanic

Fig. 3 Major element oxide variations of Camiguin lavas (*solid dots*) plotted against SiO_2 content. *Open square symbol* represents Mt. Butay gabbroic xenolith



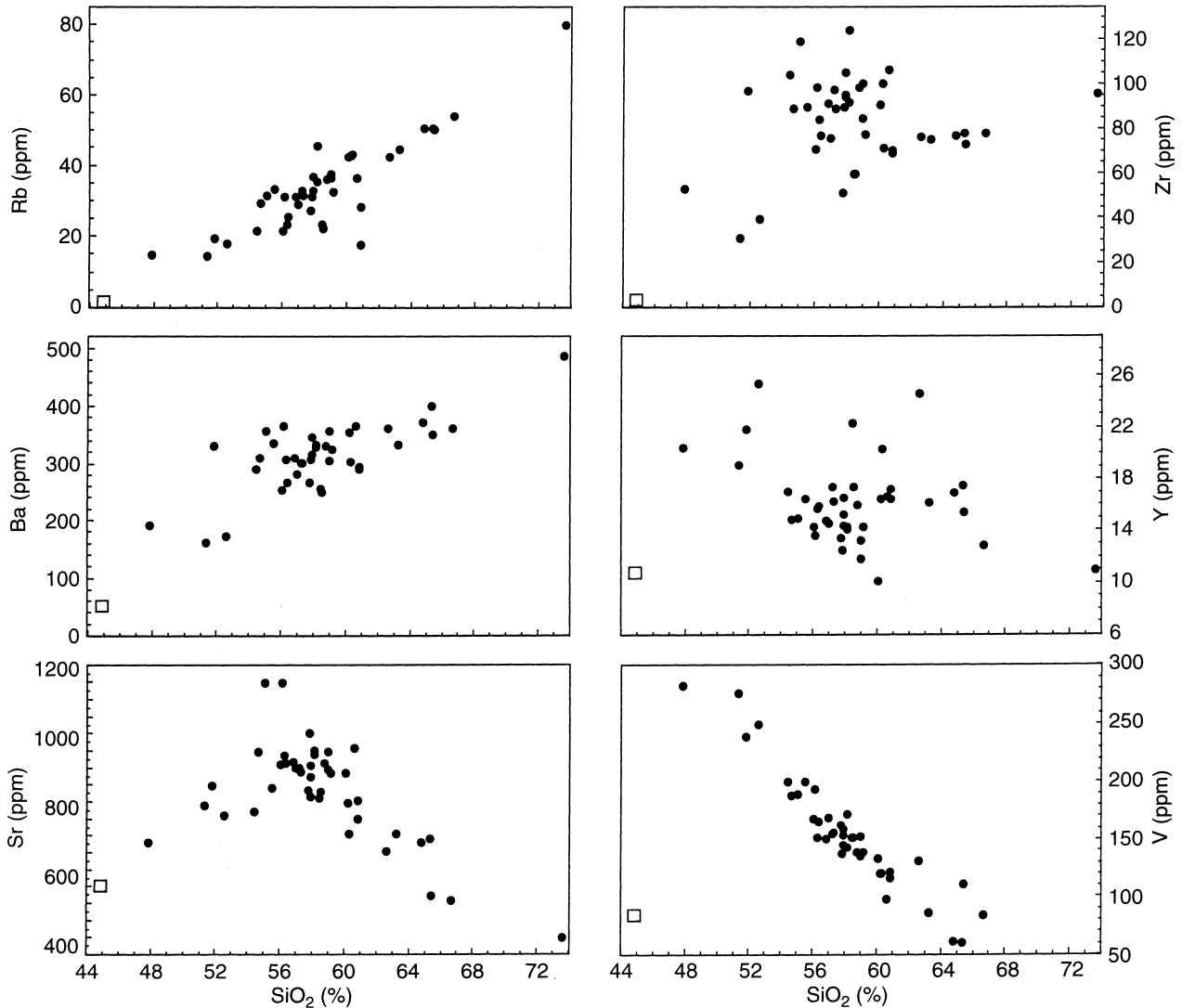


Fig. 4 Trace element variations of Camiguin lavas plotted against SiO_2 content. Symbols as in Fig. 3

eruptions (e.g., Pallister et al. 1992), producing progressively younger, more differentiated lavas at each volcano. This sequence of events ends when volcanism shifts to a new eruption center, where the cycle is repeated. The southeastern volcano (i.e., Mt. Butay) is the oldest volcanic center in the island (Punongbayan and Solidum 1985) and radiometric ages of the most mafic lavas from each volcanic center show a small but distinct increase from Mt. Butay to Mt. Hibok-hibok (Sajona et al. 1997), that is, toward the northwest, along the main trend of the CMA volcanoes in central Mindanao. The youngest constructional volcanic feature on Camiguin, the Mt. Vulcan lava dome (Fig. 1), is on the northwestern slope of Hibok-hibok and an old cemetery on the northwestern tip of the island currently lies offshore, a few meters below sea level because of on-going crustal deformation in this area.

Camiguin's relationship with the Central Mindanao Arc

The geographic and structural setting, overall young age, and northwestward migration of Camiguin volcanism are consistent with the proposal that Camiguin is the northernmost extension of the CMA (e.g., Corpuz 1992; Sajona et al. 1994, 1997). The composition of calcalkaline Camiguin lavas also overlaps to a large degree with that of the mainly medium-K calcalkaline to shoshonitic lavas in the CMA (Corpuz 1992; Sajona et al. 1993, 1994, 1997), which naturally has a wider range because central Mindanao has more numerous and larger volcanic centers as well as a thicker and more tectonically complex crust than Camiguin (e.g., Moore and Silver 1983; Hawkins et al. 1985). Although major element chemistry alone does not constitute a diagnostic feature of the source of arc lavas (e.g., Grove et al. 1982), the compositional affinity of Camiguin lavas with those of the CMA becomes more evident once the trace element and particularly the Sr, Nd and Pb isotopic data are also considered.

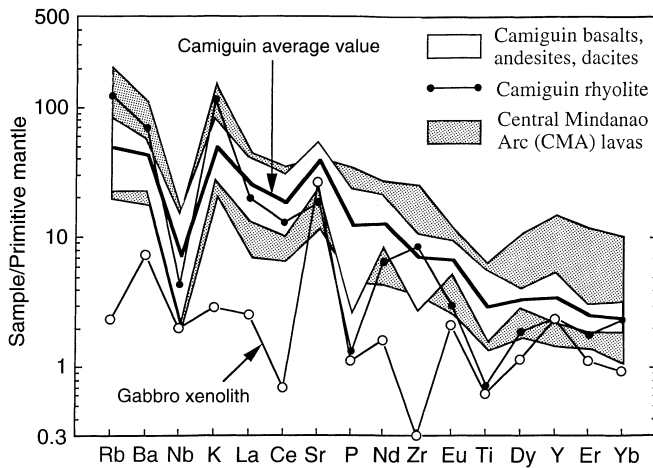


Fig. 5 Spider diagrams for Camiguin lavas compared to those for the CMA lavas (Sajona et al. 1993, 1994, 1997). Primitive mantle normalizing values from Sun and McDonough (1989)

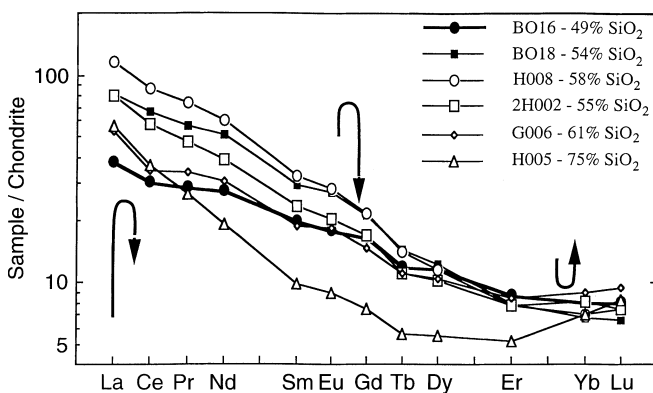


Fig. 6 Chondrite normalized REE concentration patterns for representative Camiguin lavas. Arrows show behavior of (from left to right) light-, middle-, and heavy-REE contents of lavas relative to the parental basalt BO16 with increasing differentiation. Chondrite normalizing values from Evensen et al. (1978)

Figure 5 shows that the trace element content, particularly the average value, of Camiguin basalt to dacite lavas is well within the range of the CMA basaltic to dacitic lavas. Lavas from both Camiguin and the CMA show enrichment in LILE and light-REE and depletion in HFSE and heavy-REE. The rhyolite is the only Camiguin lava that does not fit within the CMA (or even within the Camiguin) range but this is most likely the result of extreme crystal fractionation/accumulation. In detail, the similarity in trace element composition is greatest in the mafic end of Camiguin and the CMA lava series and less so in the differentiated end. For example, mafic lavas of both lava series have similar Zr/Y and Zr/Ti ratios, but the CMA differentiated lavas generally have higher Zr for given Zr/Y and Zr/Ti lavas than Camiguin differentiated lavas (Fig. 8A and B). Camiguin mafic lavas overlap with the bulk of the CMA

lavas in the La/Yb versus Sr/Y plot, but the differentiated lavas of the former extend to higher ratios than those of the latter (Fig. 8C). Finally, Camiguin and the CMA mafic lavas overlap in the La/Yb versus Ba/La plot, but the former show a slightly negative to an almost horizontal trend whereas the latter show a more variable, sub-vertical trend (Fig. 8D). All these plots suggest that the mafic lavas of both series, which are parental to the more differentiated lavas, have very similar, if not common, sources. The compositional divergence with increasing differentiation is not surprising given the differences in crustal thickness and, presumably size and depth of magma chamber beneath the CMA and Camiguin volcanoes.

A more illuminating line of evidence for the connection between the sources of Camiguin and the CMA lavas is shown by the isotopic data. The Sr and Nd isotopic composition of Camiguin lavas lies well within that of central Mindanao lavas (Fig. 7A), suggesting that Camiguin and the CMA lavas share a common source, at least in terms of these two isotopes. In detail, however, Camiguin lavas have slightly higher $^{143}\text{Nd}/^{144}\text{Nd}$ than most of the CMA lavas in accordance with the systematic latitudinal variation in the composition of the mantle source beneath southern Philippines (Castillo 1996). Lead isotopic data show this latitudinal variation more clearly. Although there is a slight overlap, Camiguin lavas have higher $^{206}\text{Pb}/^{204}\text{Pb}$ for given $^{207}\text{Pb}/^{204}\text{Pb}$ or $^{208}\text{Pb}/^{204}\text{Pb}$ than the CMA lavas; the CMA lavas show subvertical trends in the Pb-Pb isotope diagrams (Fig. 7B and C). Subvertical trends in $^{207}\text{Pb}/^{204}\text{Pb}$ and $^{208}\text{Pb}/^{204}\text{Pb}$ versus $^{206}\text{Pb}/^{204}\text{Pb}$ plots are a characteristic feature of lavas from different segments of the Philippine arc systems (e.g., McDermott et al. 1993; Mukasa et al. 1994; Castillo 1996). This may have resulted from addition of sediments with variable isotopic compositions to an isotopically homogeneous mantle wedge (McDermott et al. 1993) or to fairly recent addition of Pb from a subduction component to a mantle wedge originally variable in $^{206}\text{Pb}/^{204}\text{Pb}$ (Castillo 1996). In almost all cases, the northern part of a particular segment of the Philippine arc systems has higher $^{206}\text{Pb}/^{204}\text{Pb}$ than the southern part, consistent with Camiguin having higher $^{206}\text{Pb}/^{204}\text{Pb}$ than the CMA. Thus, in summary, isotopic data clearly support the inference that Camiguin is a northern extension of the CMA.

The origin of adakites in the Central Mindanao Arc

Melting of the down-going basaltic crust produces silica-oversaturated lavas (e.g., Rapp et al. 1991) characterized by, among other things, high Sr/Y and La/Yb ratios (> 40 and > 20 , respectively) and low Y and Yb contents ($< 15\text{--}18$ ppm and $< 1\text{--}1.5$ ppm, respectively) (e.g., Drummond and Defant 1990; Peacock et al. 1994). Drummond and Defant (1990; see also Defant and Drummond 1990; Defant et al. 1992) reported the presence of such slab-derived lavas in several arc settings

Table 3 Isotopic ratio values with analytical uncertainties (*NA* not analyzed). Measurements done at the Department of Terrestrial Magnetism (DTM) of the Carnegie Institution of Washington, except those for H005, which were done at the Scripps Institution of Oceanography (SIO). Uncertainties shown refer to the last significant figures and are instrumental in-run precisions. Analytical uncertainty, based on repeated measurements of standards at DTM for $^{87}\text{Sr}/^{86}\text{Sr}$, is ± 20 ; uncertainty for $^{143}\text{Nd}/^{144}\text{Nd}$ is ± 23 ; uncertainties on Pb isotopic ratios are approximately ± 0.015 for $^{206}\text{Pb}/^{204}\text{Pb}$ and $^{207}\text{Pb}/^{204}\text{Pb}$ and ± 0.06 for $^{208}\text{Pb}/^{204}\text{Pb}$. Analytical

| Sample | $^{87}\text{Sr}/^{86}\text{Sr}$ | $^{143}\text{Nd}/^{144}\text{Nd}$ | $^{206}\text{Pb}/^{204}\text{Pb}$ | $^{207}\text{Pb}/^{204}\text{Pb}$ | $^{208}\text{Pb}/^{204}\text{Pb}$ |
|---------------------|---------------------------------|-----------------------------------|-----------------------------------|-----------------------------------|-----------------------------------|
| B016 Mt. Butay | 0.703796 \pm 25 | 0.513006 \pm 17 | 18.287 \pm 1 | 15.545 \pm 1 | 38.243 \pm 2 |
| G001 Ginsiliban | 0.703676 \pm 25 | 0.513006 \pm 18 | 18.314 \pm 1 | 15.566 \pm 1 | 38.288 \pm 1 |
| M011 Mt. Mambajao | 0.703706 \pm 25 | 0.512973 \pm 15 | 18.307 \pm 1 | 15.532 \pm 1 | 38.192 \pm 1 |
| C03-001 Hibok-hibok | 0.703726 \pm 25 | 0.513016 \pm 8 | 18.336 \pm 1 | 15.542 \pm 1 | 38.227 \pm 1 |
| H005 Hibok-hibok | 0.703827 \pm 22 | 0.513009 \pm 18 | NA | NA | NA |
| C011 Xenolith | 0.703227 \pm 25 | 0.513021 \pm 26 | 18.367 \pm 7 | 15.601 \pm 6 | 38.346 \pm 16 |

uncertainties for Sr and Nd isotopic measurements at SIO are comparable to those at DTM. Sr isotopic ratios were fractionation-corrected to $^{86}\text{Sr}/^{88}\text{Sr} = 0.1194$ and normalized to $^{87}\text{Sr}/^{86}\text{Sr} = 0.71025$ for NBS 987. Nd isotopic ratios were measured in oxide form and fractionation-corrected to $^{146}\text{NdO}/^{144}\text{NdO} = 0.72225$ ($^{146}\text{Nd}/^{144}\text{Nd} = 0.7219$) and are reported in relation to $^{143}\text{Nd}/^{144}\text{Nd} = 0.511860$ for the La Jolla Nd Standard. Pb isotopic ratios were corrected for mass fractionation based on average measured values for NBS 981 using the values of Catanzaro et al. [1968]

and named these lavas “adakites” in special reference to the rare magnesian andesites from Adak Island in the western Aleutians. Note, however, that Kay (1978) proposed the Adak Island magnesian andesites to be magmas derived from melting of subducted Pacific sea-floor basalt which had reacted extensively with the mantle wedge prior to eruption, producing lavas that are more primitive (e.g., higher MgO, Ni and Cr content) and have slightly lower Sr/Y and La/Yb than “true” adakites. Similarly, Yogodzinski et al. (1995) proposed that the “Adak-type” magnesian andesites in the extreme western Aleutians are not true slab melts but rather magmas derived from the mantle wedge *metasomatized* by melts of subducted basalts.

Recently, Peacock et al. (1994) showed that among the proposed locations of recent adakites, only Cook Island and Cerro Pampa in southernmost Chile, Mount St. Helens in the U.S. and El Valle in Panama fit the theoretical thermal structure needed for partial melting of subducted hydrated basalt, with southernmost Chile being the least controversial. In this region, the magnesian andesites of Cook Island and andesites and dacites of the Cerro Pampa volcanic center have the distinctive chemistry and Sr, Nd and Pb isotopic characteristic of a slab-derived melt with little or no participation from either subducted sediment or the fairly thin (< 35 km) continental crust (e.g., Stern and Kilian 1996; Kay et al. 1993). More recently, Schiano et al. (1995) reported possible remnants of melts of a subducted basaltic crust, preserved as inclusions trapped within, and as interstices between, minerals in mantle xenoliths from Batan Island, one of the volcanoes in the northern segment of the western Philippine island arc (Fig. 1). The materials in the inclusions and interstices are glassy, and hence, most likely represent liquid compositions, and they have the chemical signatures expected for melts derived by low-degree melting of a subducted metabasalt at the garnet amphibolite-eclogite transition (Schiano et al. 1995). Thus, the geochemical signatures of adakites from southernmost Chile and Batan silicic glasses, together with western Aleutian magnesian andesites, provide

powerful constraints for identifying melts from subducted basaltic crust and from mantle wedge influenced by subducted basalt melt in other arc regions, including the Philippine arc setting.

Sajona and co-workers (Sajona et al. 1993, 1994, 1997; Maury et al. 1996) identified the andesites and dacites ($\text{SiO}_2 > 56$ wt%) with high Sr/Y and La/Yb ratios erupted together with voluminous basaltic to dacitic calcalkaline lavas in the eastern, central and western arcs in Mindanao as adakites. Those in the western arc are formed by melting of the young Miocene Sulu Sea crust, whereas those in the eastern arc result from initiation of subduction along the Philippine Trench (Fig. 1). In the CMA, Sajona and co-workers proposed the adakites to be products of melting of a remnant lithosphere detached from the Molucca Sea plate at 4–5 Ma due to the closing of the collision zone between the Halmahera and Sangihe arcs in central Mindanao (Pubellier et al. 1991). Sajona and co-workers claimed that relatively high Sr/Y and La/Yb ratios and low Y and Yb contents of the adakites are difficult to produce directly from the CMA calcalkaline basalts through normal differentiation processes. In their study, they analyzed lavas that were collected in temporally and spatially separated volcanic centers in the CMA, and were not able to sample a complete spectrum of lavas from individual volcanic centers.

In this study, we argue that the CMA lavas identified as adakites were derived through fractionation of more mafic lavas and that there are no “true” adakites or basaltic crust-derived melts in the CMA. This conclusion is based on the following reasons: (1) Our investigation of Camiguin represents the most detailed investigation that has ever been done on any volcanic center in the CMA. In addition, Camiguin lavas have a more pristine composition than the CMA lavas in central Mindanao because the former were injected directly through the oceanic crust whereas the latter must have additionally intruded previously erupted island arc complexes and the Cretaceous to Paleogene basement consisting of ophiolitic and greenschist facies metavol-

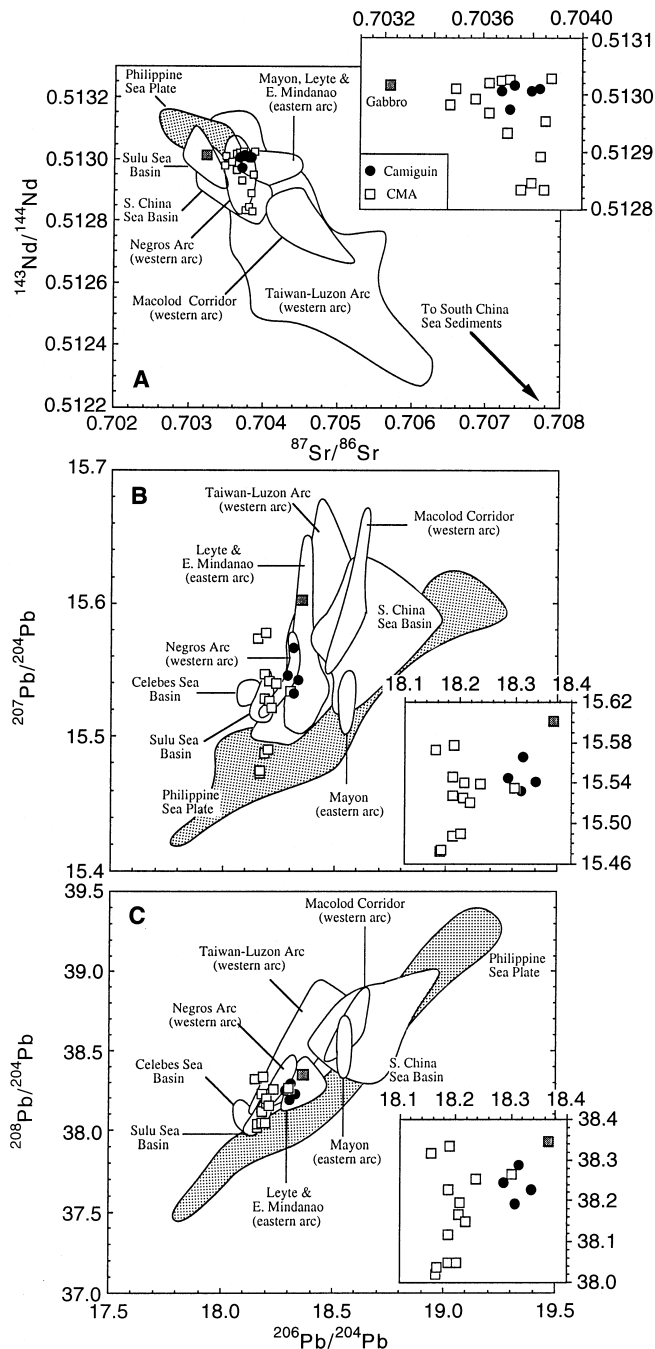


Fig. 7 Plot of: **A** $^{87}\text{Sr}/^{86}\text{Sr}$ versus $^{143}\text{Nd}/^{144}\text{Nd}$; **B** $^{206}\text{Pb}/^{204}\text{Pb}$ versus $^{207}\text{Pb}/^{204}\text{Pb}$; **C**: $^{206}\text{Pb}/^{204}\text{Pb}$ versus $^{208}\text{Pb}/^{204}\text{Pb}$ ratios of Camiguin lavas and gabbro xenolith, and central Mindanao lavas relative to other arc lavas from the Philippines. Central Mindanao data from Castillo (1996 and unpublished) and P.R. Castillo and F.G. Sajona (unpublished data)

canic rocks (e.g., Hawkins et al. 1985; Villamor and Marcos 1981). Results of our investigation strongly suggest that the Camiguin andesites and dacites that have high Sr/Y and La/Yb ratios and low Y and Yb contents (e.g., samples M022, M029, H010; Table 1 and Figs. 9A and B), that is, those that are very similar to the purported adakites in Mindanao, can be derived from

mixtures of the more mafic and differentiated lavas through AFC processes. (2) Both the Camiguin differentiated lavas and the CMA adakites (as well as the other Mindanao adakites) do not have the extremely high Sr/Y and La/Yb ratios possessed by the more likely slab-derived lavas from southernmost Chile, high-silica glass inclusions from Batan Island and the magnesian andesites from Adak Island (Fig. 9B). Moreover, Camiguin differentiated lavas and most of the Mindanao adakites plot at the extension of the normal basalt-andesite-dacite association of Camiguin and the CMA (Fig. 9A and B), suggesting that these adakite-like lavas can simply be related to the other arc rock types through shallow level fractionation processes, as is the case in Camiguin. (3) The CMA adakites are spatially and temporally coeval with basaltic lavas derived from the mantle wedge (Sajona et al. 1997). This means that the CMA adakites must have passed through a mantle wedge that is capable of melting to produce basaltic melts, and thus, is hotter than that necessary to produce silicic slab melts. Hence, it is difficult to imagine that the CMA adakites were able to survive interactions with hot mantle peridotite without losing their distinctive slab-derived chemical signature as they rise through the overlying mantle wedge (e.g., Kelemen et al. 1993). (4) All samples analyzed from both Camiguin (this study) and the CMA (Sajona et al. 1993, 1994, 1997; Maury et al. 1996) are crystalline, variably phyrlic rocks that do not represent true liquid compositions. In particular, the variable fractionation of plagioclase and amphibole phenocrysts could easily increase or decrease the bulk concentrations of Sr and La relative to Y and Yb in these rocks (e.g., Fig. 9c). (5) Finally, the presence of accessory phases such as zircon and apatite in the CMA high-silica lavas (Sajona et al. 1993, 1994) suggests that these could have variably fractionated from the lavas. Even a small amount of fractionation of these phases could easily deplete the heavy-REE and other moderately incompatible trace element contents in the high-silica lavas, giving them trace element characteristics similar to adakites. In other words, petrographic data strongly suggest that it is possible to have a small proportion of lavas that have adakite-like trace element characteristics and appear distinct from other CMA lavas although they are petrogenetically related.

Constraining the source of parental arc lavas in Camiguin and the Central Mindanao Arc

In addition to forming adakite lavas, Sajona and co-workers proposed that subducted basalt-derived melts metasomatized the mantle wedge to produce the more voluminous calcalkaline and shoshonitic basalt-andesite-dacite lava series in the CMA. However, results of our investigation are more consistent with the mantle wedge source of Camiguin lavas being metasomatized mainly by fluids dehydrated primarily from the sedimentary section of the subducted slab. This conclusion is based partly on the fact that both Camiguin and the

Table 4 Petrogenetic modeling results. The basic equation for the open system AFC used is: $C_m = C_o F^{-z} + \frac{x C_o + y C_i}{z} (1 - F^{-z})$ where the C_s represent elemental concentrations in the daughter magma (C_m), the parent (C_o), the assimilated (C_i), and the intruding magma (C_j). The terms x , y and z are functions of the ratios of rates of crystallization, intrusion and eruption and the bulk distribution coefficient. F is the ratio of the initial to final magma mass, which is 1 for a magma chamber of constant size (Reagan et al. 1987). The AFC model requires that the ratios of the rates of assimilation (R_a), crystallization (R_c), intrusion (R_i) and eruption (R_e) be known. R_d/R_c , R_i/R_c and R_e/R_c ratios are all assumed to be zero in the pure crystal fractionation models. In the mixing-crystallization models the R_d/R_c ratio is calculated from the ratio of the mass of B016 “mafic parental melt” to the mass of crystallized phases used in each least-squares model, and R_e/R_c and R_i/R_c are assumed to be zero. Partition coefficient sources are: REE – Luhr and Carmichael (1980), Zr, Sr and Rb – Gill (1981), and Y – Pearce and Norry (1979). (bas basalt, dac dacite, rhy rhyolite)

| Major element models | Model #1 | | Model #2 | | | | |
|-----------------------------|--|--|--|--|---|---|---|
| | Mixing + crystallization | | Mixing + crystallization | | | | |
| | B016 (bas) + B017 (dac) → B018 (and) | B016 (bas) → B018 (and) | B016 (bas) + H005 (rhy) → B017 (dac) | B016 (bas) → B017 (dac) | | | |
| Parental composition | B016 B017 | 72.8% 27.2% | 100% | B016 H005 | 52.7% 47.3% | 100.0% | |
| Melt fraction remaining (F) | | 0.65 | 0.21 | F | 0.74 | 0.15 | |
| Fractionating assemblage | Olivine Clinopyroxene Plagioclase Hornblende Titanomagnetite | 7.2% 56.3% 32.7% | 14.6% 33.9% 45.7% | Olivine Clinopyroxene Plagioclase Hornblende Titanomagnetite | 11.0% 24.8% 10.6% 53.5% | 5.9% 13.0% 29.3% 49.3% 2.5% | |
| Error | $\Sigma(r^2)$ | 0.0799 | 0.7786 | $\Sigma(r^2)$ | 0.0705 | 0.3344 | |
| Trace element models | | | | | | | |
| Element | Actual concentration | Mixing + fractionation Modeled concentration | Pure fractionation Modeled concentration | Actual concentration | Mixing + fractionation Modeled concentration | Pure fractionation Modeled concentration | |
| | La Ce Nd Zr Y Sr Rb | 20.1 42.5 24.3 104 16.9 769 21.6 | 22.4 40.2 21.7 108 18.9 775 47.0 | 36.9 75.6 44.2 219.5 53.8 734 61.5 | 17.2 26.3 14.3 77.5 17.4 692 50.3 | 14.6 26.1 12.3 91.0 15.0 561 68.0 | 48.6 86.8 34.6 205.7 40.0 1201 85.2 |
| Partition coefficients: | La | Ce | Nd | Zr | Y | Sr | Rb |
| Olivine | 0.01 | 0.01 | 0.01 | 0.01 | 0.01 | 0.01 | 0.01 |
| Clinopyroxene | 0.14 | 0.20 | 0.50 | 0.20 | 1.0 | 0.10 | 0.04 |
| Hornblende | 0.14 | 0.30 | 0.80 | 0.50 | 1.0 | 0.20 | 0.05 |
| Plagioclase | 0.13 | 0.12 | 0.08 | 0.01 | 0.06 | 2.0 | 0.15 |
| Titanomagnetite | 0.22 | 0.12 | 0.25 | 0.15 | 0.2 | 0.01 | 0.01 |

CMA mafic lavas generally do not share chemical characteristics with Adak Island primitive magnesian andesite lavas, which are lavas derived from melts of subducted Pacific seafloor basalt that reacted with the mantle wedge (Kay 1978; Yogodzinski et al. 1995), and mainly on mixing model calculations using trace element data, as will be shown below.

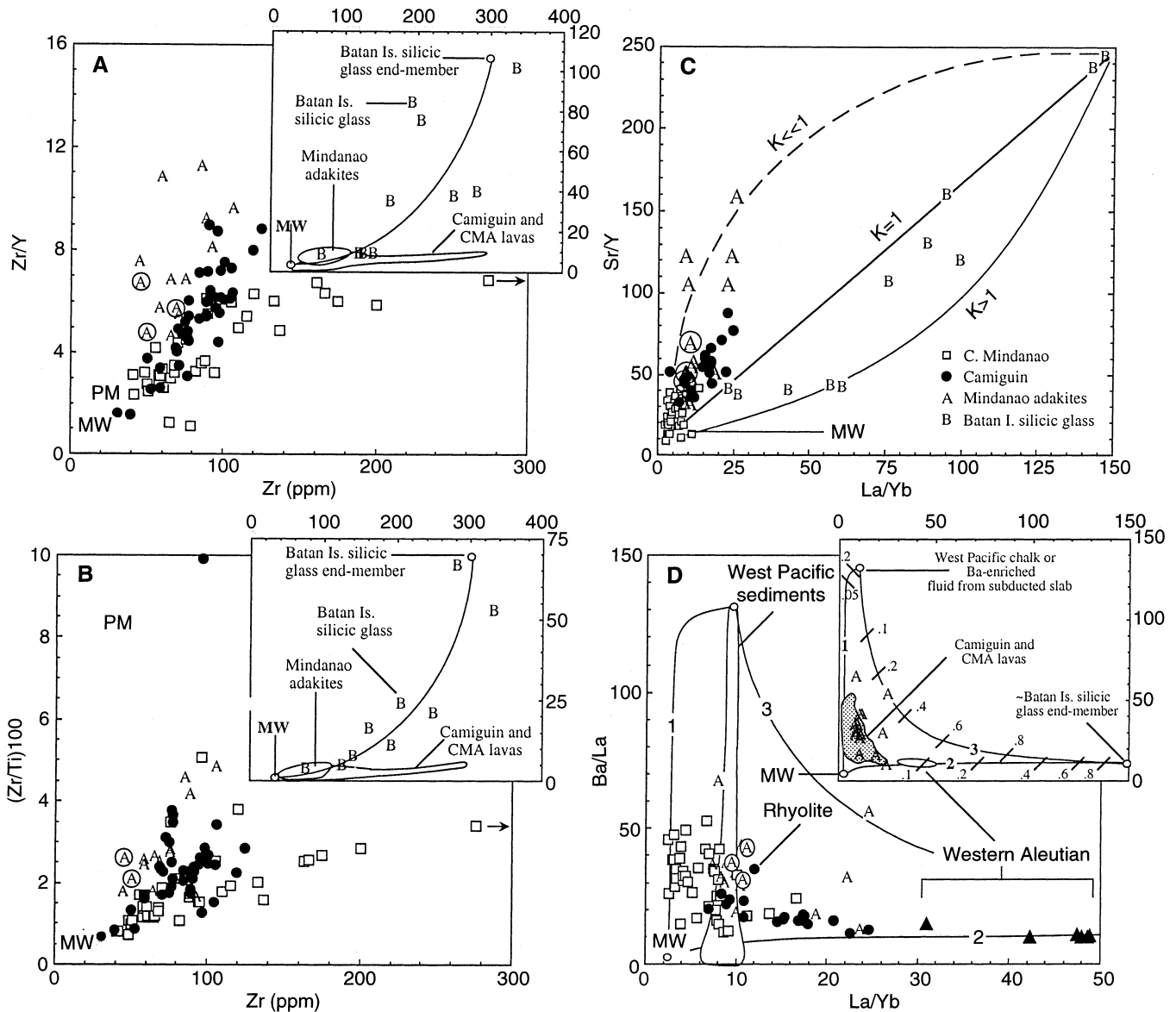
Schiano et al. (1995) proposed that the Batan Island glass inclusions in xenoliths with high-silica content represent low-degree melts of the subducted basaltic crust whereas the host Batan andesites represent higher degree melt generated from the mantle wedge previously metasomatized by the basaltic crust-derived high-silica melt; interstitial glasses in xenoliths with intermediate silica content represent a mixture between these two end-member melt compositions. Thus, the complete chemical spectrum of Batan silicic glass inclusions and interstitial glasses provides a unique guide for tracing the liquidus composition of lavas produced by mixing basaltic crust melt and melt from a mantle wedge metasomatized by basaltic crust melt. Based on HFSE data, Camiguin and the “normal” CMA lavas as well as Mindanao adakites overlap with such a mixing curve (Figs. 8A and B). However, the amount of basaltic crust melt needed to produce the mafic lavas and adakites is fairly small, and more importantly, this model does not take into account any increase in Zr, Zr/Y or Zr/Ti due simply to crystal fractionation of Camiguin and the CMA magmas. Indeed, the La/Yb versus Sr/Y plot (Fig. 8C) illustrates that the influence of basaltic crust melt on the petrogenesis of the mafic lavas is questionable, to say the least. In this plot, the K value of the mixing curve [where $K = (Y/Yb)_{\text{mantle wedge}} / (Y/Yb)_{\text{basaltic melt}}$; e.g., Langmuir et al. 1978] produced by the Batan Island silicic glasses is greater than or equal to 1. On the contrary, Camiguin lavas, the normal CMA lavas and all Mindanao adakites have much lower La/Yb for given Sr/Y ratio requiring that the subducted basalt source of CMA adakites has a different Y/Yb ratio than the source of the Batan Island silicic glass. Hence, we believe that the Sr/Y versus La/Yb variations of Camiguin, CMA lavas and all Mindanao adakites are due to normal differentiation processes rather than due to mixing processes in the source.

Finally, mixing models involving La/Yb versus Ba/La (Fig. 8D) are not only inconsistent with the idea that basaltic melt influences the mantle wedge, but they also indicate that it is most likely fluid dehydrated from subducted sediments that interacts with or metasomatizes the mantle wedge to produce mafic lavas that are parental to both Camiguin and the CMA lavas. Barium is enriched in many oceanic sediments (e.g., Kay 1980; Lin 1991; Plank and Langmuir 1993) and is relatively poor in the altered basaltic section of the oceanic crust (e.g., Weaver 1991; Staudigel et al. 1996) and in the depleted upper mantle (e.g., Ewart and Hawkesworth 1987). Experimental results have shown that Ba is extremely mobile in fluids during hydrothermal dehydration of subducted sediments (You et al. 1996) and

altered basalts (e.g., Kogiso et al. 1997; Brenan et al. 1995) such that Ba is strongly enriched in slab-derived fluids. It has also been shown that Ba/La in arc lavas correlates fairly well with $^{10}\text{Be}/^9\text{Be}$ and B/La (Leeman et al. 1994), both of which are most likely controlled by subduction of young sediments (e.g., Morris et al. 1990). Thus, based on these arguments, the source of primitive arc lavas coming from the mantle wedge was most likely influenced by Ba-enriched fluids dehydrated from the subducted slab or by melts of sediments with extremely high Ba/La such as the west Pacific chalk (Lin 1991). Note that direct melting of bulk West Pacific sediments (Lin 1991) may not necessarily produce high Ba/La arc lavas as these sediments have fairly low (~ 13) Ba/La ratio.

Camiguin lavas show an almost horizontal to slightly negative trend in the Ba/La against La/Yb plot (Fig. 8B). Interestingly, the high La/Yb and low Ba/La end of the trend consists mainly of basaltic andesites and andesites whereas the low La/Yb and high Ba/La end consists mainly of andesites and dacites as well as the most primitive basalt (La/Yb = 7; Ba/La = 20). This is consistent with the REE behavior discussed earlier (Fig. 6) that the La/Yb ratio of the lavas initially increases and then decreases with increasing fractionation. In other words, although it probably has nothing to do with melting of a subducted basaltic crust, the Camiguin fractionation array trends toward the fields for adakites and lavas from slab-melt metasomatized mantle wedge. On the other hand, the normal CMA lavas generally have low La/Yb (most < 10) but with high and variable Ba/La. Almost all Mindanao adakites (CMA adakites are circled) are similar to the normal CMA lavas in terms of Ba/La and only a few have high La/Yb (> 10) values.

Collectively, the sources of Camiguin and the CMA mafic lavas have higher Ba/La and La/Yb ratios than a simple multiply depleted mantle wedge (Ba/La = 4; La/Yb = 0.3). Their source most likely is the mantle wedge that has been metasomatized with a component with relatively high Ba/La and La/Yb ratios. Of course, an alternative explanation is that the mafic lavas were simply produced from the mantle wedge by a very low extent of melting to give them their high Ba/La and La/Yb ratios, but many other studies of convergent margin magmatism (e.g., Gill 1981; Ewart and Hawkesworth 1987; Tatsumi et al. 1991; Maury et al. 1992; Kogiso et al. 1997) clearly suggest that this can not be the cause of the high ratios. The field for the mafic lavas, particularly those from the CMA, overlaps with the mixing curve between the mantle wedge and a high Ba/La sediments/fluids component released from the slab (Curve # 1 in Fig. 8D) but plots above the mixing curve between the mantle wedge and the basaltic melt (Curve # 2). This suggests that the high Ba/La and relatively low La/Yb component that metasomatized the mantle wedge most likely comes from subducted sediment/dehydrated fluid rather from a basaltic melt. The mixing curves also indicate that it is highly unlikely that any of the other



adakites in Mindanao reported by Sajona and co-workers (1993, 1994, 1997) are pure melts of subducted basalt. A few of the Mindanao adakites that have high Ba/La plot along or close to Curve # 3, indicating their sources or parental basaltic melts must have mixed with subducted sediment or dehydrated fluid prior to eruption.

That the mantle wedge was metasomatized by a component released from subducted sediments is highly consistent with the subvertical trends of Camiguin, the CMA and many other Philippine arc lavas in Pb-Pb isotopic ratio plots (Figs. 7B and C). These subvertical trends most likely represent mixing of the mantle wedge with variable $^{206}\text{Pb}/^{204}\text{Pb}$ ratios with a component released from the subducted slab having high $^{207}\text{Pb}/^{204}\text{Pb}$ and $^{208}\text{Pb}/^{204}\text{Pb}$ for a given $^{206}\text{Pb}/^{204}\text{Pb}$ ratio, which is most likely the upper sedimentary section of the slab (Castillo 1996; McDermott et al. 1993). Such a high

$^{207}\text{Pb}/^{204}\text{Pb}$ and $^{208}\text{Pb}/^{204}\text{Pb}$ isotopic signature of the component could not have come from the basaltic crust alone because altered basaltic crust has lower $^{207}\text{Pb}/^{204}\text{Pb}$ ratios than subducted sediments (Miller et al. 1994; Brenan et al. 1995).

To briefly summarize, model calculations using the Batan Island silicic glasses and western Aleutian magnesian andesites collectively to represent basaltic crust melt and mixture of basaltic crust melt and mantle wedge indicate that the main source of mafic lavas of Camiguin and the CMA is not subducted basaltic crust, nor a mantle wedge metasomatized by melts from a subducted basaltic crust. Rather, these mafic lavas appear to be mainly a product of a multi-depleted mantle wedge metasomatized by fluids mainly derived from dehydration of subducted sediments. This notion is highly consistent with the Pb isotopic data, which show a strong sediment (or more appropriately, sediment-de-

Fig. 8 Plots of: **A** Zr concentration versus Zr/Y; **B** Zr versus (Zr/Ti) *100; **C** Sr/Y versus La/Yb; **D** Ba/La versus La/Yb for Camiguin lavas, normal CMA lavas, Mindanao adakites (CMA adakites are circled), Batan Island silicic glasses and Adak Island high-magnesian andesites (whenever data are available – Yogodzinski et al. 1995). *PM* represents the primitive mantle (Sun and McDonough 1989); *MW* represents estimated composition of the mantle wedge, and field for west Pacific sediments is from Lin (1991) with a west Pacific chalk having the extreme Ba/La composition. In the *insets* in **A** and **B**, *curves* show mixing possibilities between mantle wedge and slab melt represented by the Batan Island silicic glasses inside xenoliths with the highest Zr and SiO₂ values (Schiano et al. 1995). In **C**, the *solid curve* and *straight line* represent mixing relationship between a pure slab melt, represented by a Batan Island silicic glass with the highest Sr/Y and La/Yb ratios, and the metasomatized mantle wedge. The curvatures of these curves, determined by the $K = (Y/Yb)_{\text{mantle wedge}} / (Y/Yb)_{\text{basaltic melt}}$ ratio or *K*, are $> 0 = 1$. Mindanao adakites have much less La/Yb for given Sr/Y ratio than Batan Island silicic glasses. If Mindanao adakites also represent slab melts (or more appropriately, slab melts mixed with the metasomatized mantle wedge), then the curvature of their mixing curve (*dashed*) is $\ll 1$. *Inset* in plot **D** illustrates possible mixing relationships among the mantle wedge and West Pacific chalk (or sediment-derived fluid with high Ba/La – *curve 1*), subducted basalt melt and West Pacific chalk (or sediment-derived fluid with high Ba/La – *curve 2*) and subducted basalt melt and mantle wedge (*curve 3*). *Tick marks* on *curve 1* represents proportions of chalk (or fluid) in the mixture whereas those in *curves 2 and 3* represent proportions of subducted basalt melt. In all plots, Mindanao adakites, particularly those from the CMA (circled), plot close to the mantle wedge rather than the slab melt. More discussion in the text

ried component) imprint. Based on these results we conclude that, although we cannot completely rule out melting of subducted basaltic crust beneath the CMA, the role of basaltic melt in generating CMA lavas is relatively minor.

Summary and conclusions

Camiguin island is comprised of four stratovolcanoes that have produced basaltic to rhyolitic lavas. Camiguin lavas are medium-K, calcalkaline and generally form coherent major element trends on SiO₂ variation diagrams with no significant differences between volcanoes except for the extent of differentiation. Trace element data also show that Camiguin lavas have a typical calcalkaline arc signature: LILE and light-REE enriched and HFSE and heavy-REE depleted. Chemical and isotopic data indicate that all Camiguin lavas share a single mantle source. Petrogenetic modeling of major and trace elements suggests that Camiguin lavas were produced by an AFC process in which fractional crystallization is accompanied by the occasional reinjection of parental melt into the magma chamber and subsequent mixing of differentiated and parental magmas.

Tectonic, major and trace element, and Sr, Nd, and Pb isotopic data suggest that Camiguin is an extension of the tectonically complex CMA. The most likely source of the CMA and Camiguin parental magmas is the mantle wedge metasomatized by fluids dehydrated from subducted sediments and oceanic crust. Some

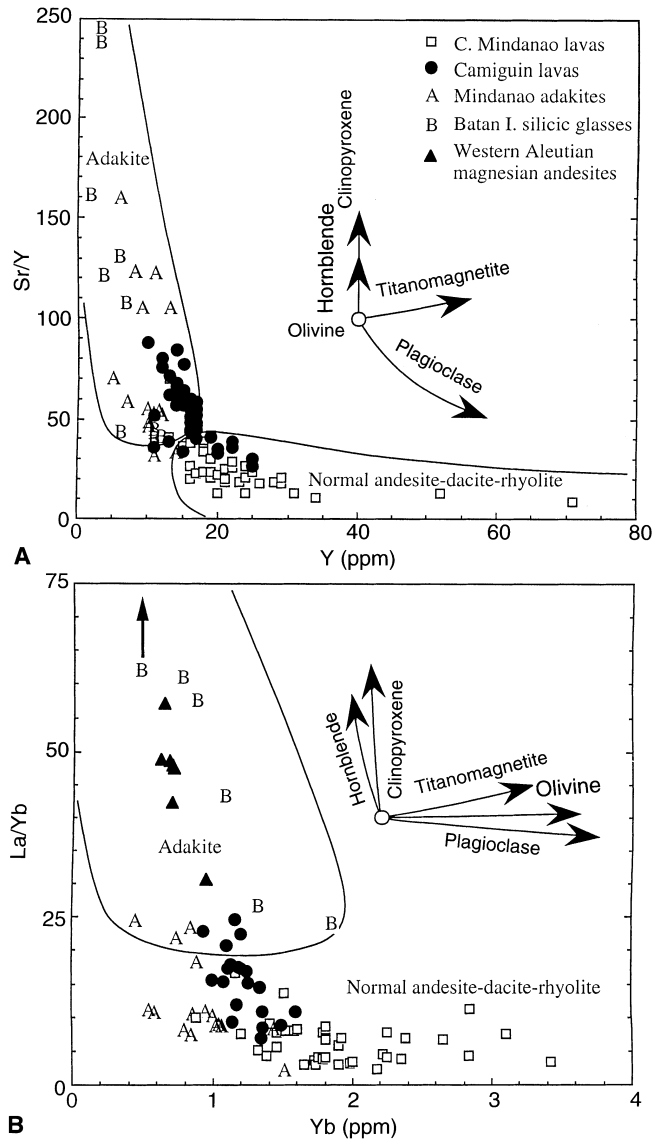


Fig. 9 Plots of: **A** Sr/Y versus Y; **B** La/Yb versus Y for Camiguin lavas, CMA lavas, Mindanao adakites (CMA adakites are circled), Batan Island silicic glasses and western Aleutian high-magnesian andesites. Adakite fields are based on the geochemical characteristics of lavas presumed derived from partial melting of subducted basaltic crust (e.g., Defant and Drummond 1990; Drummond et al. 1997), magnesian andesites from western Aleutian (Kay 1978; Yogodzinski et al. 1995), and Batan Island silicic glasses (Schiano et al. 1995). Crystal fractionation paths of the primary minerals are indicated by *arrows* for reference. More discussion in the text

Camiguin high-silica lavas are similar to Mindanao lavas which have been identified as adakites derived from direct melting of a subducted basaltic crust. However, detailed investigation indicates that CMA adakites are not pure basaltic crust melts. At most, these adakites may have been derived from a mantle wedge that had been metasomatized mainly by dehydrated fluids and to a lesser extent by basaltic crust melts. However, it is most likely that the CMA adakites, like Camiguin high-silica lavas, are simply products of an AFC process.

Acknowledgements We are grateful to Director R.S. Punongbayan for the logistical support afforded us during fieldwork in Camiguin, to F.F. Florendo for assistance in the analyses of lavas, and to S.M. Kay, T.P. Wagner and T.L. Grove for constructive reviews. This work is supported by NSF grants INT91-96017 and EAR93-13571 and Carnegie Institution of Washington Postdoctoral Fellowship to P.C.

References

- Acharya HK, Aggarwal YP (1980) Seismicity and tectonics of the Philippine Islands. *J Geophys Res* 85: 3239–3250
- Atherton MP, Petford N (1993) Generation of sodium-rich magmas from newly underplated basaltic crust. *Nature* 362: 144–146
- Baker DR (1987) Depths and water content of magma chambers in the Aleutian and Mariana island arcs. *Geology* 15: 496–499
- Baker DR, Eggler DH (1983) Fractionation paths of Atka (Aleutians) high-alumina basalts: constraints from phase relations. *J Volcanol Geothermal Res* 18: 387–404
- Besana GM, Negishi H, Ando M (1997) The three-dimensional attenuation structures beneath the Philippine archipelago based on seismic intensity data inversion. *Earth Planet Sci Lett* 151: 1–11
- Brenan JM, Shaw HF, Ryerson FJ, Phinney DL (1995) Mineral-aqueous fluid partitioning of trace elements at 900 °C and 2.0 GPa: constraints on the trace element chemistry of mantle and deep crustal fluids. *Geochim Cosmochim Acta* 59: 3331–3350
- Castillo PR (1996) The origin and geodynamic implication of the Dupal isotopic anomaly in volcanic rocks from the Philippine island arcs. *Geology* 24: 271–274
- Castillo PR, Carlson RW, Batiza R (1991) Origin of Nauru Basin igneous complex: Sr, Nd and Pb isotope and REE constraints. *Earth Planet Sci Lett* 103: 200–213
- Catanzaro EL, Murphy TJ, Shields WR (1968) Absolute isotopic abundance ratios of common, equal-atom, and radiogenic lead isotopic standards. *J Res Natl Bur Stand* 72 A
- Corpuz ESG (1992) Petrology and geochemistry of the Central Mindanao Volcanic Arc, southern Philippines. PhD thesis, Univ Canterbury
- Defant MJ, Drummond MS (1990) Derivation of some modern arc magmas by melting of the subducted lithosphere in a volcanic arc. *Nature* 347: 662–665
- Defant MJ, De Boer JZ, Oles D (1988) The western Central Luzon volcanic arc, the Philippines: two arcs divided by rifting? *Tectonophysics* 145: 305–317
- Defant MJ, Jacques D, Maury RC, De Boer J, Joron J (1989) Geochemistry and tectonic setting of the Luzon arc, Philippines. *Geol Soc Am Bull* 101: 63–672
- Defant MJ, Jackson TE, Drummond MS, De Boer JZ, Bellon H, Feigenson MD, Maury RC, Stewart RH (1992) The geochemistry of young volcanism throughout western Panama and southeastern Costa Rica: an overview. *J Geol Soc London* 149: 569–579
- DePaolo DJ (1981) Trace element and isotopic effects of combined wall rock assimilation and fractional crystallization. *Earth Planet Sci Lett* 53: 189–202
- Drummond MS, Defant MJ (1990) A model for trondhjemite-tonalite-dacite genesis and crustal growth via slab-melting: Archean to modern comparison. *J Geophys Res* 95: 21503–21521
- Drummond MS, Defant MJ, Kepezhinskas PK (1996) Petrogenesis of slab-derived trondhjemite-tonalite-dacite/adakite magmas. *Trans R Soc Edinburgh Earth Sci* 87: 205–215
- Evensen N, Hamilton PJ, O’Nions RK (1978) Rare-earth abundances in chondritic meteorites. *Geochim Cosmochim Acta* 42: 1199–1212
- Ewart A, Hawkesworth CJ (1987) The Pleistocene–Recent Tonga–Kermadec arc lavas: interpretation of new isotopic and rare earth data in terms of depleted mantle source model. *J Petrol* 28: 495–530
- Förster H, Oles D, Knittel U, Defant MJ, Torres RC (1990) The Macolod Corridor: a rift crossing the Philippine island arc. *Tectonophysics* 183: 265–271
- Gill JB (1981) Orogenic andesites and plate tectonics. Springer-Verlag, Berlin Heidelberg New York Tokyo
- Green TH, Pearson NJ (1985) Experimental determination of REE partition coefficients between amphibole and basaltic liquids at high pressure. *Geochim Cosmochim Acta* 49: 1465–1468
- Grove TL, Gerlach DC, Sando TW (1982) Origin of calc-alkaline series lavas at Medicine Lake Volcano by fractionation, assimilation and mixing. *Contrib Mineral Petrol* 80: 160–182
- Hall R (1996) Reconstruction of Cenozoic SE Asia. In: Hall R, Blundell D (eds) *Geol Soc Spec Publ* 106: 153–184
- Hamilton W (1979) Tectonics of the Indonesian region. USGS Prof Pap 1078
- Hawkins JW, Moore GF, Villamor R, Evans C, Wright E (1985) Geology of the composite terranes of East and Central Mindanao. In: Howell D (ed) *Earth science series*, 1. pp 437–463. Circum-Pacific Council for Energy and Mineral Resources, Houston, TX, USA.
- Janney PE, Castillo PR (1996) Basalts from the Central Pacific Basin: evidence for the origin of Cretaceous igneous complexes in the Jurassic Western Pacific. *J Geophys Res* 101: 2875–2894
- Janney PE, Castillo PR, Baker PE (1995) Petrology and geochemistry of basaltic clasts and hyaloclastites from volcanoclastic sediments at Site 869. *Ocean Drilling Program Proc Sci Results* 143: 263–276
- Kay RW (1978) Aleutian magnesian andesites: melts from subducted Pacific ocean crust. *J Volcanol Geothermal Res* 4: 117–132
- Kay RW (1980) Volcanic arc magmas: implications of a melting-mixing model for element recycling in the crust-upper mantle system. *J Geol* 88: 497–522
- Kay SM, Gordillo CE (1994) Pocho volcanic rocks and the melting of depleted continental lithosphere above a shallowly dipping subduction zone in the central Andes. *Contrib Mineral Petrol* 117: 25–44
- Kay RW, Kay SM (1993) Delamination and delamination magmatism. *Tectonophysics* 219: 177–189
- Kay SM, Ramos VA, Marquez M (1993) Evidence in Cerro Pampa volcanic rocks for slab-melting prior to ridge-Trench Collision in South America. *J Geol* 101: 703–714
- Kelemen PB, Shimizu N, Dunn T (1993) Relative depletion of niobium in some arc magmas and the continental crust: partitioning of K, Nb, La and Ce during melt/rock reaction in the upper mantle. *Earth Planet Sci Lett* 120: 111–134
- Knittel U, Defant MJ (1988) Sr isotopic and trace element variations in Oligocene to Recent igneous rocks from the Philippine island arc: evidence for recent enrichment in the sub-Philippine mantle. *Earth Planet Sci Lett* 87: 87–99
- Kogiso T, Tatsumi Y, Nakano S (1997) Trace element transport during dehydration processes in the subducted oceanic crust. 1. Experiments and implications for the origin of oceanic island basalts. *Earth Planet Sci Lett* 148: 193–205
- Langmuir CH, Vocke R, Hanson G, Hart S (1978) A general mixing equation with application to Icelandic basalts. *Earth Planet Sci Lett* 37: 380–392
- Leeman WP, Carr MJ, Morris JD (1994) Boron geochemistry of the Central American volcanic arc: constraints on the genesis of subduction related magmas. *Geochim Cosmochim Acta* 58: 149–168
- Le Maitre RW (1981) GENMIX – a generalized petrological mixing model program. *Comput Geosci* 7: 229–247
- Lin P-N (1991) Trace element and isotopic characteristics of western Pacific pelagic sediments: implications for the petrogenesis of Mariana Arc magmas. *Geochim Cosmochim Acta* 56: 1641–1654
- Lindsley (1983) Pyroxene thermometry. *Am Mineral* 68: 477–493

- Luhr JF, Carmichael ISE (1980) The Colima Volcanic Complex, Mexico. 1. Post-caldera andesites from Volcan Colima. *Contrib Mineral Petrol* 71: 343–372
- Martin H (1986) Effect of steeper Archean geothermal gradient on geochemistry of subduction-zone magmas. *Geol* 14: 753–756
- Maury RC, Defant MJ, Joron J-L (1992) Metasomatism of the sub-arc mantle inferred from trace elements in Philippine xenoliths. *Nature* 360: 661–663
- Maury RC, Sajona FG, Pubellier M, Bellon H, Defant M (1996) Fusion de la croûte océanique dans les zones de subduction/collision récentes: l'exemple de Mindanao (Philippines). *Bull Soc Geol Fr* 167: 579–595
- McDermott F, Defant MJ, Hawkesworth CJ, Maury RC, Joron JL (1993) Isotope and trace element evidence for three component mixing in the genesis of the North Luzon arc lavas (Philippines). *Contrib Mineral Petrol* 113: 9–23
- Miklius A, Flower MFJ, Huijsmans JPP, Mukasa SB, Castillo PR (1991) Geochemistry of lavas from Taal Volcano, southwestern Luzon, Philippines: evidence for multiple magma supply systems and mantle source heterogeneity. *J Petrol* 32: 593–627
- Miller DM, Goldstein SL, Langmuir CH (1994) Cerium/lead and lead isotopic ratios in arc magmas and the enrichment of lead in the continents. *Nature* 368: 514–520
- Moore GF, Silver EA (1983) Collision processes in the northern Molucca Sea. In: Hayes DE (ed), *Am Geophys Union Monogr* 27: 360–372
- Morris JD, Leeman WP, Tera F (1990) The subducted component in island arc lavas: constraints from Be isotopes and B-Be systematics. *Nature* 344: 31–36
- Mukasa SB, McCabe R, Gill JB (1987) Pb-isotopic compositions of volcanic rocks in the west and east Philippine island arcs: presence of the Dupal isotopic anomaly. *Earth Planet Sci Lett* 84: 153–164
- Mukasa SB, Flower FJ, Miklius A (1994) The Nd-, Sr- and Pb-isotopic character of lavas from Taal, Laguna de Bay and Arayat volcanoes, S.W. Luzon, Philippines: implications for arc magma petrogenesis. *Tectonophysics* 235: 205–221
- Newhall CG (1979) Temporal variation in the lavas of Mayon Volcano, Philippines. *J Geophys Res* 6: 61–83
- Norrish K, Chappell B (1977) X-ray fluorescence spectrometry. In: Zussman J (ed) *Physical methods in determinative mineralogy*, Academic Press, New York, pp 201–272
- Norrish K, Hutton JT (1969) An accurate X-ray spectrographic method for the analysis of a wide range of geological samples. *Geochim Cosmochim Acta* 33: 431–453
- Pallister JS, Hoblitt RP, Reyes AG (1992) A basalt trigger for the 1991 eruptions of Pinatubo volcano? *Nature* 356: 426–428
- Peacock SM, Rushmer T, Thompson AB (1994) Partial melting of subducting oceanic crust. *Earth Planet Sci Lett* 121: 227–244
- Pearce JA, Norry MJ (1979) Petrogenetic implications of Ti, Zr, Y and Nb variations in volcanic rocks. *Contrib Mineral Petrol* 69: 33–47
- Plank T, Langmuir CH (1993) Tracing trace elements from sediment input to volcanic output at subduction zones. *Nature* 362: 739–743
- Pubellier M, Quebral R, Tangin C, Deffontaines B, Muller C, Butterlin J, Manzano J (1991) The Mindanao collision zone: a soft collision event within a continuous Neogene strike-slip setting. *J Southeast Asian Earth Sci* 6: 239–248
- Punongbayan RS, Solidum RU (1985) Camiguin Island. *Philipp Inst Volcanol Seismol*, Quezon City, Philippines
- Rapp RP, Watson EB, Miller CF (1991) Partial melting of amphibolite/eclogite and the origin of Archean trondhjemites and tonalites. *Precambrian Res* 51: 1–25
- Reagan MK, Gill JB, Malavassi E, Garcia MO (1987) Changes in magma composition at Arenal volcano, Costa Rica, 1968–1985: real-time monitoring of open system differentiation. *Bull Volcanol* 49: 415–434
- Sajona FG, Maury RC, Bellon H, Cotten J, Defant MJ, Pubellier M, Rangin C (1993) Initiation of subduction and the generation of slab melts in western and eastern Mindanao, Philippines. *Geology* 21: 1007–1010
- Sajona FG, Bellon H, Maury RC, Pubellier M, Cotten J, Rangin C (1994) Magmatic response to abrupt changes in geodynamic settings: Pliocene-Quaternary calc-alkaline lavas and Nb-enriched basalts of Leyte and Mindanao (Philippines). *Tectonophysics* 237: 47–72
- Sajona FG, Maury RC, Bellon H, Cotten J, Defant MJ (1996) High field strength element enrichment of Pliocene-Pleistocene island arc basalts, Zamboanga Peninsula, western Mindanao (Philippines). *J Petrol* 37: 693–726
- Sajona FG, Bellon H, Maury RC, Pubellier M, Quebral RD, Cotten J, Bayon FE, Pagado E, Pamatian P (1997) Tertiary and Quaternary magmatism in Mindanao and Leyte (Philippines): geochronology, geochemistry and tectonic setting. *J Asian Earth Sci* 15: 121–153
- Schiano P, Clocchiatti R, Shimizu N, Maury RC, Jochum KP, Hofmann AW (1995) Hydrous, silica-rich melts in the sub-arc mantle and their relationship with erupted arc lavas. *Nature* 377: 595–600
- Smith TE, Huang CH, Sajona FG (1991) Geochemistry and petrogenesis of basalts from Holes 767C, 770B, and 770C, Celebes Sea. In: Silver EA, Rangin C, von Breyman MT, et al. (eds) *Proc Ocean Drilling Program* 124, pp 311–320
- Spadea P, D'Antonio M, Thirlwall MF (1996) Source characteristics of the basement rocks from the Sulu and Celebes Basins (Western Pacific): chemical and isotopic evidence. *Contrib Mineral Petrol* 123: 159–176
- Staudigel H, Plank T, White W, Schmincke H-U (1996) Geochemical fluxes during seafloor alteration of the basaltic upper oceanic crust; DSDP sites 417 and 418. In: Bebout GE, Scholl DW, Kirby SH, Platt JP (eds) *Subduction top to bottom*. *Am Geophys Union Monogr* 96, pp 19–38
- Stern CR, Kilian R (1996) Role of the subducted slab, mantle wedge and continental crust in the generation of adakites from the Andean Austral Volcanic Zone. *Contrib Mineral Petrol* 123: 263–281
- Sun S-S, McDonough WF (1989) Chemical and isotopic systematics of oceanic basalts: implications for mantle composition and processes. In: Saunders AD, Norry MJ (eds) *Magmatism in the ocean basins*. *Geol Soc Spec Publ* 42, pp 313–345
- Tatsumi Y, Murasaki M, Arsadi EM, Nohda S (1991) Geochemistry of Quaternary lavas from Southeast Sulawesi: transfer of subduction components into the mantle wedge. *Contrib Mineral Petrol* 107: 137–149
- Villamor R, Marcos DM (1981) Preliminary report on the geology of Tankulan, Dumalaguing, Sumilao and Kalasungay quadrangles. *Phillipp Bur Mines Geosci Reg Off X*
- von Biedersee H, Pichler H (1995) The Canlaon and its neighboring volcanoes in the Negros Belt/Philippines. *J Southeast Asian Earth Sci* 10: 1–13
- Walker RJ, Carlson RW, Shirley SB, Boyd FR (1989) Os, Sr, Nd and Pb isotope systematics of southern African peridotite xenoliths: implications for the chemical evaluation of subcontinental mantle. *Geochim Cosmochim Acta* 53: 1583–1595
- Weaver B (1991) The origin of ocean island basalt end-member compositions: trace element and isotopic constraints. *Earth Planet Sci Lett* 104: 364–397
- Yogodzinski GM, Kay RW, Volynets ON, Koloskov AV, Kay SM (1995) Magnesian andesite in the western Aleutian Komandorsky region: implications for slab melting and processes in the mantle wedge. *Geol Soc Am Bull* 107: 505–519
- You C-F, Castillo PR, Chan LH, Gieskes JM, Spivack AJ (1996) Trace element behavior in hydrothermal experiments: implications for fluid processes at shallow depths in subduction zones. *Earth Planet Sci Lett* 140: 41–52